Evaluation of self-welding susceptibility of austenitic stainless steel (alloy D9 and 316LN) in high temperature flowing sodium

By

C. MEIKANDAMURTHY

Enrollment no ENGG 02200804004

Indira Gandhi centre for Atomic Research

Kalpakkam 603102

A Thesis submitted to

Board of studies in Engineering Sciences

In Partial fulfillment to the requirements of

for the Degree

Doctor of Philosophy

Of

Homi Bhabha National Institute

December 2012

Homi Bhabha National Institute

Recommendations of the Viva Voce Committee

As members of the Viva Voce Board, we certify that we read the dissertation prepared by **C. Meikandamurthy** entitled " **Evaluation of self-welding susceptibility of austenitic stainless steel (alloy D9 and 316LN) in high temperature flowing sodium"** and recommend that it may be accepted as fulfilling the dissertation requirement for the degree of **Doctor of Philosophy**.

---------------------------------- Date:
Chairperson Dr. B. P. C. Rao

---------------------------------- Date:
Convener/Guide Dr Shaju K. Albert

---------------------------------- Date:
Member-1 External Examiner

----------------------------------- Date:
Member-2 Dr. G. Amarendra

------------------------------------ Date:
Member-3 Dr. M. Sai Baba

-------------------------------------- Date:
Tech. advisor Shri K. K. Rajan

Final approval and acceptance of this dissertation is contingent upon the candidate's submission of final copies of the thesis to HBNI.

I hereby certify that I have read this thesis prepared under my direction and recommend that it may be accepted as fulfilling the thesis requirement.

Date: 02/01/15

Place: Kalpakkam

Guide (Dr Shaju K. Albert)

STATEMENT BY AUTHOR

This dissertation has been submitted in partial fulfillment to the requirements for an advanced degree at Homi Bhabha National Institute (HBNI) and is deposited in the library to be made available to borrowers under the rules of HBNI.

Brief quotations from this dissertation are allowable without special permission provided that accurate acknowledgement of source is made. Requests for permission for extended quotation from or reproduction of this manuscript in whole or in part may be granted by competent authority of HBNI when in his or her judgment the proposed use of the materials in the interest scholarship. In all other instances, permission must be obtained from the author.

C. Meikandamurthy

DECLARATION

I, hereby declare that the investigation presented in the thesis titled **"Evaluation of self-welding susceptibility of austenitic stainless steel (alloy D9 and 316LN) in high temperature flowing sodium"** has been carried out by me**.** The work is original and has not been submitted earlier as a whole or in part for a degree / diploma at this or any other institution / University**.**

C. Meikandamurthy

LIST OF PUBLICATIONS ARISING FROM THE THESIS

Journal

1. *Self-welding susceptibility of 316LN and alloy D9 stainless steel in high temperature flowing sodium* **Meikandamurthy C**, Hemant Kumar, Albert S.K, Ramakrishnan V, Rajan K.K and Bhaduri A.K Int Journal Nuclear Energy Science and Technology 2010 Vol.5 No.3 pp 195-206

2. *Effect of cold-work on self-welding susceptibility of austenitic stainless steel (alloy D9) in high temperature flowing sodium* **Meikandamurthy C,** Hemant Kumar, Gopa Chakraborty, Albert S.K, Ramakrishnan V, Rajan K.K and Bhaduri A.K Journal of Nuclear Materials 2010 Vol 407 165-170

3. *Self-welding susceptibility of cold-worked alloy D9 and 316LN austenitic steel in flowing sodium* **Meikandamurthy C**, Hemant Kumar, Gopa Chakraborty, Albert S.K, Ramakrishnan V, Chandramouli S, Rajan K.K and Bhaduri A.K. Material science and Technology 2012 vol 28 No 12 1484-1491

4. *Evaluation of Self-welding susceptibility of austenitic stainless steel (alloy D9) in sodium*, Hemant Kumar, Albert S.K, Ramakrishnan V, **Meikandamurthy C**, Amarendra G and Bhaduri A.K, Journal of Nuclear Materials, 2008 vol 374 1-8

CONFERENCES

1. Hemant Kumar , Ramakrishnan V, Rajan Babu V, Vijayashree R, Albert, S.K, Sritharan R, **Meikandamurthy C**, Balasubramaniyan V, Bhaduri, A.K *In-sodium Tribological Studies Pertaining to Core and Reactor Assembly Components for PFBR* DAE-BRNS theme meeting on Nuclear Tribology, BARC, Mumbai, Oct 2007

2. Hemant Kumar, **Meikandamurthy C**, Ramakrishnan V, Albert S.K, Chandermouli S, Bhaduri A.K, *Influence of cold-working on galling behaviour of 15Cr-15Ni-2Mo titanium modified austenitic stainless steel in liquid sodium.* NMD-ATM 2010, 64st Annual technical meeting, The Indian institute of science, 14-16th Nov 2010, Bangalore

3. Hemant Kumar, Ramakrishnan V, **Meikandamurthy C**, Albert S.K, Bhaduri A.K *Influence of high temperature sodium on galling behaviour of 15Cr-15Ni-2Mo titanium modified austenitic stainless steel.* NMD-ATM 2007, 61st Annual technical meeting, The Indian Institute of Metals, 15-16th Nov 2007, Mumbai

4. Hemant Kumar, Ramakrishnan V, **Meikandamurthy C**, Albert S.K, Bhaduri A.K, *Galling behaviour austenitic stainless steel. in high temperature liquid sodium* NMD-ATM 2009, 63rd Annual technical meeting, The Indian institute of metals, 16-17th Nov 2009, Kolkata
5. Hemant Kumar, Ramakrishnan V, **Meikandamurthy C**, Albert S.K, Bhaduri A.K, *Sliding wear and friction behaviour of 15Cr-15Ni-2Mo titanium modified austenitic stainless steel in high temperature liquid sodium.* Second Int conference on advanced tribology, Singapore 2008

3. INTERNAL TECHNICAL REPORTS

1. Hemant Kumar, Albert S.K, Bhaduri A.K, **Meikandamurthy C** *Need for hard facing coatings on Wrapper pads of fuel* subassemblies PFBR/30000/GN/1052 April 2004
2. Hemant kumar, Ramakrishnan V, **Meikandamurthy C,** Albert S.K, Bhaduri A.K, *In-sodium self-welding susceptibility studies of materials*

combination between bottom plates of grid plate and core support structure; PFBR/31000/ex/1077 Nov 2007

3. Hemant Kumar, Ramakrishnan V, **Meikandamurthy C,** Albert S.K, Bhaduri A.K *In sodium tribology studies on hardfaced material combinations of core and reactor assembly components-Experimental plan and current status.* PFBR/31000/EX/1058 R-B, Sept 2005

4. Hemant Kumar, Albert S.K ,Ramakrishnan V, **Meikandamurthy C,** Bhaduri A.K *Self-welding, friction and wear between hardfaced materials combinations of core and reactor assembly components*; IGC//HFTF/2005/03; Sep2005

5. Ramakrishnan V, Hemant Kumar, **Meikandamurthy C,** Albert S.K, Bhaduri A.K *Status report on Tribology studies*; FRTG/STG/PES/99114/EX/3014/R-B; Aug 2005

6. Hemanth Kumar, Ramakrishnan V, **Meikandamurthy C,** Albert S.K, Bhaduri A.K *In-sodium self-welding susceptibility studies between materials of wrapper pads of fuel subassemblies*; PFBR/30000/EX/1059/R-A 2004

7. Hemanth Kumar, Ramakrishan V, Meikandamurthy **C,** Albert S.K, Bhaduri A.K. *Studies on self-welding, friction and wear between hardfaced materials combination of core and reactor assembly components.* IGC/HFTF/2005/03 SEP 2003.

C. Meikandamurthy

DEDICATED TO MY FAMILY

ACKNOWLEDGEMENTS

I would like to take this pleasant opportunity to express my gratitude to those who supported me during the course.

First, I am immensely grateful to my Research Guide Dr Shaju K. Albert Head, Materials Technology Division for his invaluable guidance in the right direction to complete this work.

I am thankful to members of my Doctoral Committee Dr B. P. C Rao, and Dr G. Amrendra for their useful suggestions in my research work.

Many thanks to Dr. M. Sai Baba, Associate Director, RMG for his constant encouragement during the course.

I owe my sincere thanks to Ex-Director Shri S. C. Chetal, and present Director, Dr. P. R. Vasudeva Rao allowing me to use the various facilities in IGCAR.

I am grateful to Shri K. K. Rajan, Director, FRTG for his interest in my research work. I am thankful to Dr A. K. Bhaduri, Associate Director, Metallurgy and Materials Group for valuable discussions during my research work.

I place on record my thanks to V.Ramakrishnan Head, Mechanical service section, S. Chandramouli, Head, Rig Operation Section and their colleagues for operating the sodium system to complete the experiments in time.

I acknowledge my scientific colleagues, Shri Hemant kumar and Gopa Chakraborty extending their help in specimen analysis.

C. Meikandamurthy

CONTENTS

3 **CHAPTER 3**

EXPERIMENTAL PROGRAM

I SYNOPSIS

I SYNOPSIS

In Prototype Fast Breeder Reactor (PFBR), the core subassemblies are hexagonal in shape and are supported at the bottom by grid plate. The subassemblies are provided with a pad on the six faces of the subassemblies at the top where contact is established between adjacent subassemblies. Flowing sodium at 823 K through the core removes the oxide layers from the mating surfaces of the subassembly pads and metal to metal contact take place. During reactor operation, under extreme temperature and radiation, thermal expansion and irradiation swelling are likely to exert force in the adjacent subassemblies pad. The high temperature and prolonged contact in addition to the pressure, can lead to self-welding of contact pads. This will increase the pulling load on fuel handling machine beyond the design limit at the time of refueling where the spent fuel subassemblies are taken out from the core and fresh fuel subassemblies are inserted into the core. Hence to ensure that self-welding does not occur in fuel subassemblies contact pads, experiments were initiated simulating PFBR conditions. Thereafter, a detailed study on self-welding susceptibility of alloy D9 (which is the material chosen for subassembly contact pad) was taken up and compared with 316LN (the structural material chosen for reactor construction) taken as reference material both in the annealed and 20% cold-worked condition in high temperature flowing sodium under different contact pressure and time to understand the self-welding mechanism in these materials.

Worldwide, investigators have carried out self-welding experiments on 304, 316 and 321 austenitic stainless steel. Literature survey revealed that no work has been reported on alloy D9 and 316LN. Hence these materials used in PFBR were selected for this study. The self-welding coefficient (W) is used as a measure for self-welding tendency of materials and is defined as the shear stress for breakaway per unit contact stress (shear force / contact force).

In this research work self-welding susceptibility of alloy D9 in annealed and 20% cold-worked condition have been evaluated in flowing sodium at 823 K for a contact stress range of 9.4 MPa to 24.5 MPa and for durations of 3, 4.5, 6 and 9 months. Similarly, self-welding susceptibility of 316LN was also studied in annealed and 20% cold-worked condition and compared with the results of D9.

In this experiment, a dedicated sodium facility was used which had provision for heating, cooling and circulating sodium, monitoring impurity level in sodium with plugging indicator, and purifying sodium with cold trap. The specimens tested in the experiment were hollow cylindrical stacked one above the other under compression using Belleville spring to get the required contact stress. The mating surfaces of the specimens were polished and surface roughness was maintained below 0.5 µm. Specimen assembly is then put inside the test vessel of sodium facility. Initially the specimens contact surfaces are allowed to come in contact with pure sodium flow which removes the oxide layer from the mating surface. After 24 hours the specimens are compressed by Belleville springs. The sodium loop is operated for the specified period and sodium purity is maintained by cold trapping continuously. The contact load in the specimen is also maintained uniformly using the load cell till the end of the experiment. After the experiment, the sodium is drained and test vessel is cooled to room temperature. The specimens are taken out with sodium deposits. Cleaning of specimens was carried out with alcohol. The self-welded specimen pairs are separated by a set up to measure the shear force. The tested specimens were later analyzed for self-welding using self-welding coefficient, SEM, EDS, Macro and Micro hardness.

The results indicated that the self-welding tendency is more in annealed 316LN than in 20% cold-worked 316LN which is on the expected line. On the contrary, 20% cold-worked alloy D9 showed more self-welding tendency and the annealed alloy D9 showed no self-welding. On analysis it was found that dynamic recrystallisation favoured self-welding tendency in 20% cold-worked alloy D9 and there was no dynamic recrystallisation in annealed alloy D9. The carburisation of alloy D9 in sodium resulted in the formation of TiC precipitates at the grain boundary near the surface which accelerated the dynamic recrystallisation in 20% cold-worked alloy D9. Thus 20% cold-worked alloy D9 was found to be more susceptible for self-welding in flowing sodium. It was also determined that for PFBR conditions, self-welding will not occur in 20% cold-worked alloy D9 contact pads of the subassemblies during its operation.

II LIST OF FIGURES

III LIST OF TABLES

CHAPTER 1

INTRODUCTION

1. INTRODUCTION

1.1 Overview of PFBR

The existing coal reserves in India can produce energy only for few decades [1]. India's growing energy needs can be met only by nuclear power. The Indian Atomic Energy program is to use thermal reactors and Fast Breeder Reactors to utilize natural uranium and thorium reserves to meet the future energy requirements. Hence development of Fast Breeder Reactors is gaining importance in the country. The first commercial Fast Breeder reactor in India is Prototype Fast Breeder Reactor (PFBR).

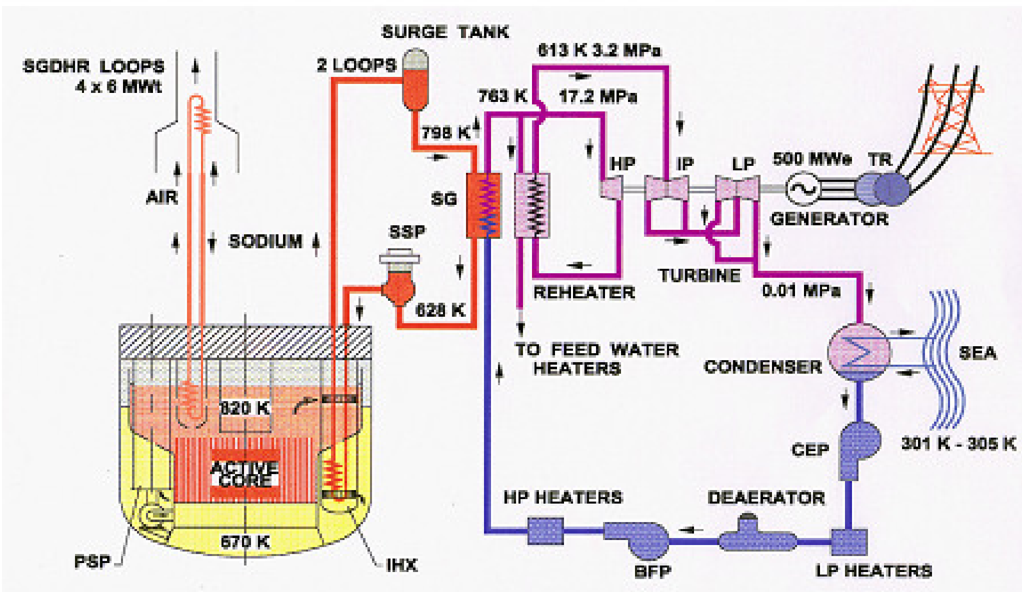

PSP	Primary sodium pump
IHX	Intermediate heat exchanger
BFP	Boiler feed pump
HP-	High Pressure
LP-	Low Pressure
TR-	Turbine

Fig. 1.1: Flow sheet of Prototype Fast Breeder Reactor [2]

Prototype Fast Breeder Reactor in India is pool type sodium cooled fast reactor [2]. The core is immersed in pool of liquid sodium as shown in Fig. 1.1. Two large primary sodium pump (PSP) circulates sodium through the core to remove heat generated due to nuclear fission. The sodium pool temperature is at about 823 K. Heat is transferred to secondary sodium circuit through intermediate heat exchanger (IHX) and secondary sodium pump (SSP). Steam is produced in steam generator SG which in turn rotates the turbo generator to produce electricity. In case of non-availability of secondary sodium loop, Safety Grade Decay Heat exchanger (SGDHR) (four in numbers) removes the decay heat to atmosphere by natural circulation of sodium. The main vessel and the components inside form the primary sodium system of PFBR. 316LN austenitic stainless steel is the major material of construction of the primary sodium system [2].

1.2. Sodium as coolant

Since a fast reactor does not have a neutron moderator such as heavy water or light water, the reactor core has to be compact resulting in very high volumetric power density. For example, the power produced in the core per unit cubic meter of a fast reactor is 550 MWt compared to an 8 MWt for a heavy water moderated reactor of the same capacity [3]. Thus it is important to use a very efficient heat transfer fluid as a coolant which should also possess favorable nuclear characteristics of low neutron moderation/absorption. Liquid metals, specifically liquid sodium, meets almost all the requirements of a fast reactor coolant due to its high thermal conductivity, reasonable specific heat, low neutron moderation and absorption and high boiling point giving a large operating temperature range at near atmospheric pressure [3]. Thus liquid sodium has all essential characteristics to be a fast reactor coolant and has been adopted in fast reactors. The high chemical activity of sodium including its violent reaction with water has been a matter of concern but the sodium technology has been mastered to circumvent the same.

1.3. Self-welding in sodium cooled fast reactors

Self-welding is a diffusion bonding phenomenon, which occurs when two smooth metallic surfaces (free of oxide layers) are pressed against each other for a particular duration at high temperature [4]. During this process, deformation of the surfaces in contact takes place (at the asperities of contact points) due to loading and during the recrystallisation that follows, diffusion of atoms takes place across the contact interface. This results in self-welding of the mating surfaces at the asperities.

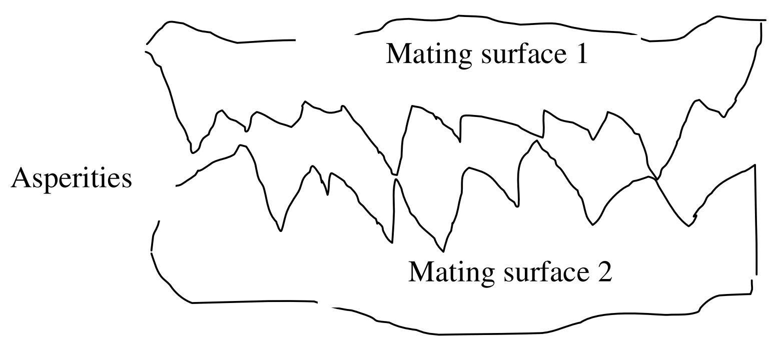

Fig. 1.2: Asperities of the mating surface

Fig.1.2 shows the asperities of the mating surface where only a few asperities come in contact and Fig.1.3 shows the progress of self-welding in asperities. The initial contact of the asperities is deformed as shown in Fig. 1.3(b) due to contact pressure and Fig. 1.3(c) shows self-welding after a specified period of time due to diffusion of atoms between the mating surfaces.

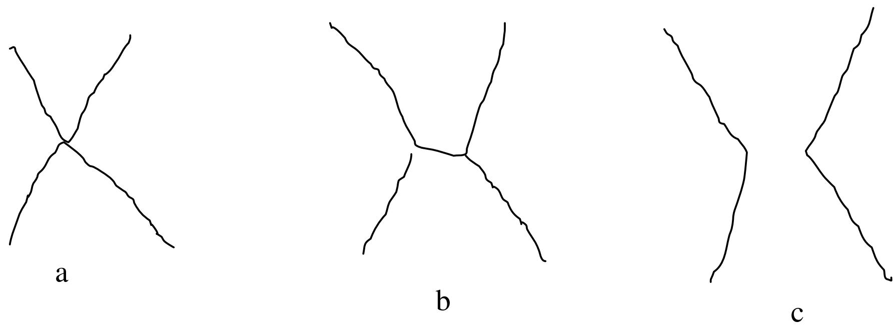

Fig. 1.3: Self-welding in asperities

In sodium cooled fast reactors, self-welding of mating surfaces of the reactor components are likely to occur as pure sodium removes the oxide layer resulting in metal to metal contact being established between the surfaces [4]. The major problems associated with self-welding are:

1. **Stuck interfaces:** Stuck interfaces may cause components to resist removal or disassembly resulting in secondary damage. (where mechanism such as control rod drive mechanism or valves would fail to operate).
2. **Surface damage to sealing surfaces:** Self-welding of valve seats to valve plugs in sodium loops may cause loss of seal across the valve seats.
3. **Ruptured components:** Unyielding bonding interface can result in stress raisers, stress ruptures and fatigue failures in nuclear components.

In many cases hard facing was done in one or both the mating surfaces to reduce self-welding susceptibility and friction [5]. Cobalt based stellite alloys, which possess excellent resistance to wear at high temperature are the natural choice as hardfacing alloys for these applications. However, in reactor environment, cobalt based alloys are not being recommended because of induced activity coming from Co^{60} isotope which is produced from n,γ reaction from its natural isotope Co^{59}. This radioactive isotope has a half-life of about 5.3 years which will lead to handling difficulties during maintenance of the components hardfaced using Co based alloys. Alterative to Co based alloys for this type of application is nickel based alloys (Colmonoy) and these are used as hardfacing material in fast breeder reactors [5]. Hard Cr plating is another process employed for protecting the surfaces against galling and self-welding [5]. Self-welding susceptibility of the chromium plated 2.25 Cr Mo steel with Inconel 82 weld metal in flowing sodium has been studied recently for fast breeder reactor application [6]. Similarly many self-welding experiments have been carried out to validate the design of hardfaced coatings and the design of the mating surface of the reactor components.

1.4. Components susceptible for self-welding in PFBR

Self-welding is a matter of concern in many components of PFBR. Table 1.1 lists some of these components and their material of construction along with operating conditions in the reactor [6]. Core subassemblies, as already mentioned, are arranged in hexagonal arrays and are supported vertically in grid plate in PFBR. Each subassembly is surrounded by six subassemblies. Contact pads are provided on each face of the hexagonal subassemblies in the top. During reactor operation, thermal expansion and swelling (irradiation induces voids in atomic structure leading to swelling in materials) of subassemblies increase the pressure contact between the contact pads. Presence of stress, high temperature and oxide free metallic surfaces, can facilitate self-welding between adjacent subassemblies at the contact surface of the pads.

In the case of grid plates, as seen from Fig. 1.4, it rests on the core support structure. As there is a difference in the sodium temperature below the grid plate, where cold sodium enters and above the grid plate, where heat is generated, there will be difference in the thermal expansion and contraction of the grid plate and the core support structure, which would result in relative movement of these massive components. To facilitate this relative movement, it is important to avoid self-welding at the location of contact between these two components. Accordingly, hardfacing using Ni base Colmonoy 5 alloy is done along two annular rings on the grid plate assembly, which form the area of contact between grid plate and core support structure.

In the primary pipe, interfaces between support plate of spherical header and support brackets from core support structure are coated with colomonoy-5 to avoid self-welding and permit relative movement of components during the operation of PFBR.

There are many more components like Control Safety Rod (CSR) subassembly, Diverse Safety Rod (DSR) subassembly, Control Safety Rod Drive Mechanism (CSRDM) and Diverse Safety Rod Drive Mechanism (DSRDM) etc, where mating surfaces encounter the risk of self-welding or wear.

All these components have been studied for their susceptibility for self-welding. However, it may be noted that in all these combinations, except in the case of core subassembly, at least one of the mating surfaces is either Cr plated or hardfaced. In the alloy D9 contact pads of the fuel subassemblies, is not hardfaced but 20% cold-worked and they are also susceptible to self-welding. The alloy D9 is 20% cold-worked to improve the resistance against radiation induced swelling [7]. Hence, it was necessary to undertake a detailed study on self-welding susceptibility of 20% cold-worked alloy D9.

Table 1.1: Material susceptible for self-welding in PFBR and the service conditions experienced by them [6]

Components	Material Combination	Temperature	Stress	Duration	Surface Finish	Medium
Core Subassembly	20%CW* D9 and 20%CW* D9	850K (normal operation) 473K (fuel handling)	1.8–3.3 MPa (normal operation) 1.6–2.7 MPa (fuel handling)	2 years	<0.8 µm	Sodium
Grid Plate	Colmonoy 5 and 316LN	673K (normal operation) 473K (fuel handling) 803K (transient condition)	≤ 11 MPa	40 years	0.8 µm	Sodium
Primary Pipe	Colmonoy 5 and Colmonoy 5	673K (normal operation) 473K (fuel handling) 803K (transient condition)	≤11 MPa	40 years	0.8 µm	Sodium
CSR Subassembly	Colmonoy 5and Cr-plated	845 K	6 MPa	8 months	0.8 µm	Sodium

Components	Material Combination	Temperature	Stress	Duration	Surface Finish	Medium
	316LN					
	Z6 NCT DV 25-15 and Colmonoy 5	845 K	60 MPa	8 months		
	Nimonic 80A and Colmonoy 5	670K (normal operation) 473K (handling)	11 MPa	2 years	0.4 µm vs. 0.8 µm	Sodium
DSR Subassembly	Cr-plated 2.25Cr-1Mo and Inconel 82	773K (normal operation) 473K (fuel handling)	1.6 MPa (normal operation) 2.4 MPa (fuel handling)	8 months	< 0.8 µm	Sodium
	Nimonic 80A and Colmonoy 5	670K (normal operation) 473K (handling)	11 MPa	2 years	0.4 µm vs. 0.8 µm	
CSRDM	Colmonoy 5 and Cr-plated 316LN	845K (lower guide) 403K (upper guide)	187 N (cylinder in cylinder) 93 N (cylinder in cylinder)	2 days	0.4 µm 0.4 µm	Sodium, Argon /
DSRDM	Colmonoy 5 and. Cr-plated 316LN	845K (lower guide) 403K (upper guide)	187 N (cylinder in cylinder) 93 N (cylinder in cylinder)	8 months	0.4 µm 0.8µm (Cr plated)	Sodium

CW* cold-worked

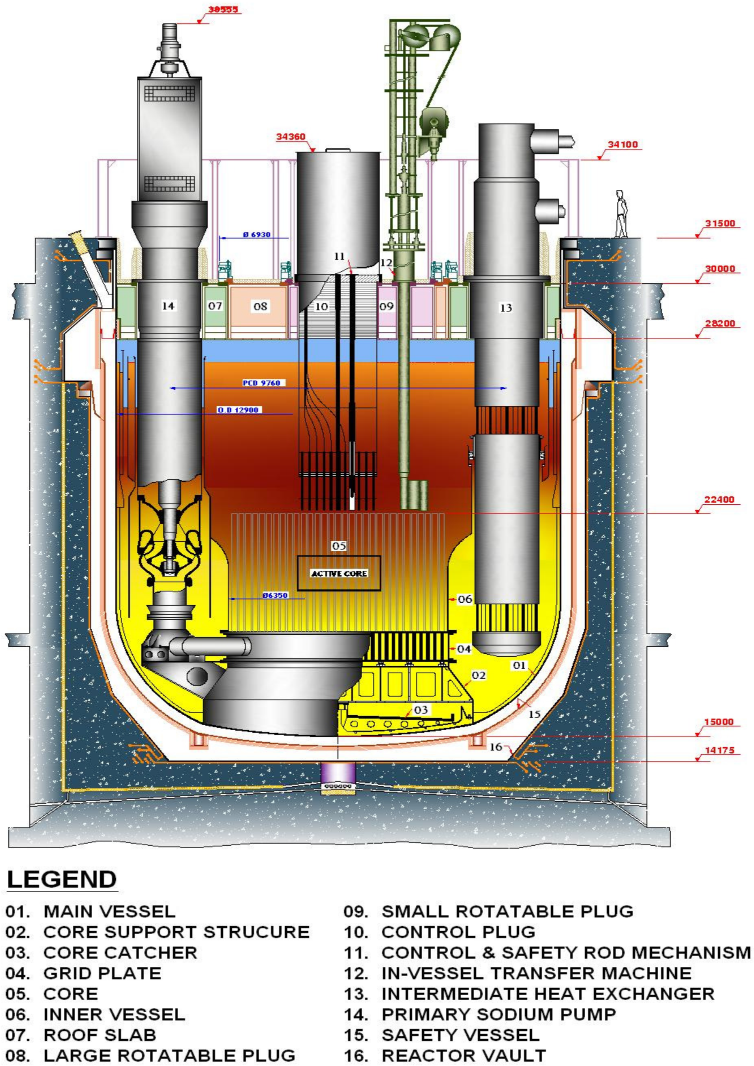

Fig. 1.4: Prototype Fast Breeder Reactor [2]

1.5. The PFBR core

Fig. 1.4 shows the vertical section of PFBR and Fig. 1.5 shows the plan view of the subassemblies of the reactor core. Subassemblies are hexagonal tubes which contain fuel, blanket (for breeding), reflector or shielding material. There are 1757 subassemblies in the PFBR core.

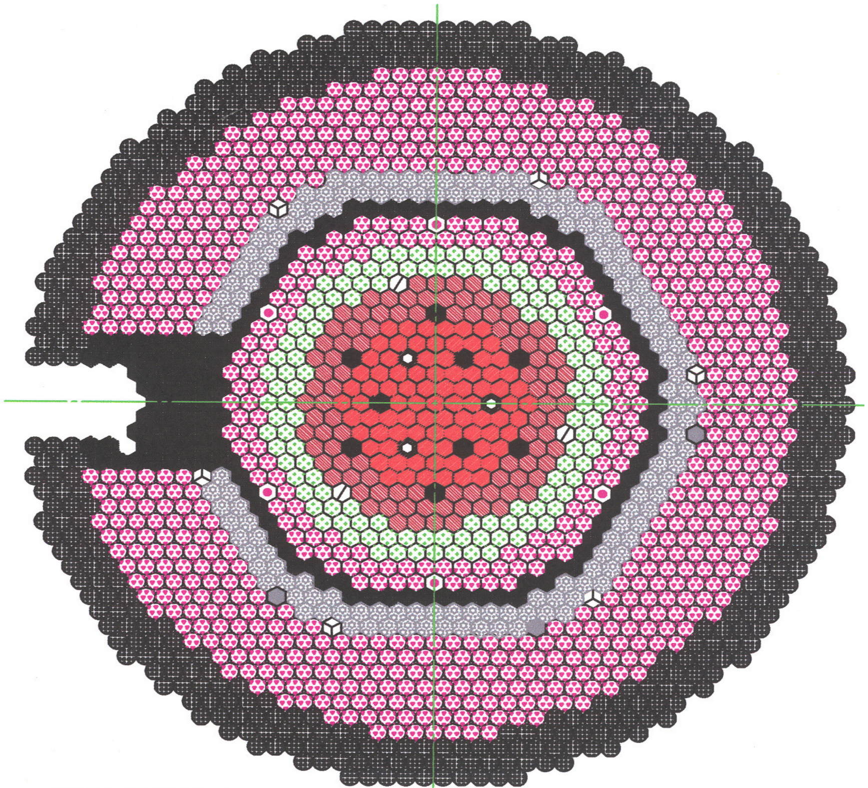

SYMBOL	TYPE OF SUBASSEMBLY	No.	MASS PER SUBASSY. IN kg
	FUEL (INNER)	85	245
	FUEL (OUTER)	96	245
	CONTROL AND SAFETY ROD	9	200
	DIVERSE SAFETY ROD	3	180
	BLANKET	117	320
	SOURCE	3	200
	STEEL REFLECTOR	132	355
	PURGER	6	355
	B_4C SHIELDING (INNER)	124	181
	STORAGE LOCATION	147	245/320/355
	STORAGE FOR SOURCE	3	200
	FAILED FUEL STORAGE LOCATION	6	245
	STEEL SHIELDING	609	330
	B_4C SHIELDING (OUTER)	417	265
	TOTAL SUBASSEMBLIES	1757	

Fig. 1.5: Plan view of the subassemblies in the core of the reactor [2]

The fuel subassemblies are surrounded by blanket, steel reflector and shielding subassemblies. Maximum heat is generated in the fuel subassemblies. Each subassembly is 4 m in height and the foot of the subassemblies is held in the sleeves provided in the grid plate at the bottom of the core. Storage location is provided for the spent fuel subassemblies to reduce the radioactivity level. All the fuel handling inside the reactor is done by Transfer Arm which locks with the subassembly head for removing or inserting fuel subassemblies in the core during refueling [8,9]. In PFBR, there are 181 fuel subassemblies and each fuel subassembly contains 217 fuel pins of 6.6 mm outside diameter (Fig.1.6). Sodium flows through the space available between the fuel pins to remove the heat produced by nuclear fission. The six sides of the subassemblies are provided with contact pads at the top so that contact between adjacent subassemblies occurs only at these pads. The material for subassemblies and fuel pin clad is alloy D9, an austenitic stainless with 15Cr-15Ni-2Mo with Ti addition. This alloy is chosen for its better resistance to radiation swelling than 316LN, the major structural material chosen for the reactor [10, 11].

1.6. Self-welding in fuel subassemblies

As already explained in the previous section, the PFBR core is compact core and the fuel subassemblies will bend against adjacent subassemblies due to swelling by radiation and thermal expansion as shown in Fig. 1.6 during the operation of the reactor. It is to be noted that the material of construction of wrapper and its pad is 20% cold-worked alloy D9. As the flowing sodium removes the oxide layer, metallic surface is exposed, making it highly susceptible to self-welding. The life of the subassemblies in the reactor is 2 years [2]. The high contact stress that could be experienced by the pad for long duration while in service at a fairly high temperature of 823 K increases the chances of self-welding occurring at the contact pads of the subassemblies. If the contact pads are self-welded removal of fuel subassemblies during refueling would be difficult as the load requirement required to separate the self-welded subassemblies might exceed the design load of fuel handling machine.

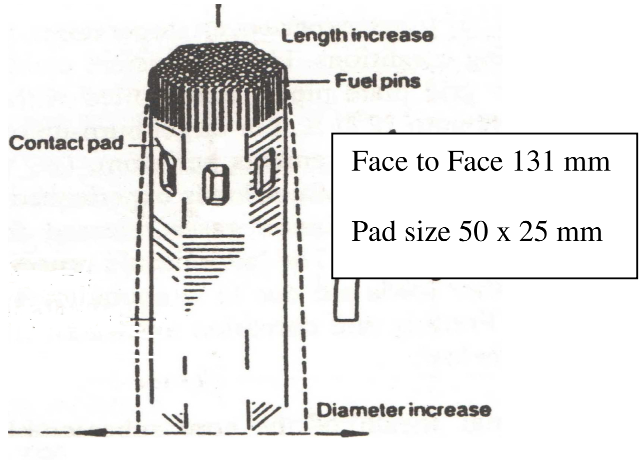

Fig. 1.6: Fuel subassembly of PFBR [10]

Providing wear resistant coatings at the contact pad locations has been reported in various FBR designs. The contact pads of subassemblies in Fast Flux Test Facility in USA, were coated with chromium carbide particles and Ni-Cr alloy (which acts as a binder), and the process employed for deposition is Detonation Gun (D-Gun) technique [12]. In PFR design of UK, the contact pads were made separately using stellite alloys and welded to 20% cold-worked PE 16 alloy (the wrapper material) by electron beam welding. In SNR-300 of Germany stellite along with Inconel 718 was chosen as hard facing material in the wear pads of subassemblies. In Indian Fast Breeder Test Reactor (FBTR), hard chrome plating is used in the 20% cold-worked 316L of fuel subassembly pads to prevent self-welding. The Rapsodie of France also had similar coating on the wrapper.

In PFBR, hard chrome plating is not proposed in the contact pads of subassemblies. The operating temperature of the core is 833 K and hard chrome plating loses its hardness significantly with increase of temperature above 723K [12]. Chromium carbide coating was also not considered as the bonding produced by D-gun process is not metallurgical in nature and there is always a risk of spalling of the coating due to weakening of the bond interface under irradiation environment and the secondary stresses generated during reactor operations. Strict dimensional tolerances specified for the subassemblies could not be met in the attempts to weld separate contact pads made of hardfacing alloy like Colmonoy to the subassemblies as in the design of UK's PFR. Further, it is also argued that 20% cold-work of alloy D9 has much higher hardness and strength than the solution annealed material and hence there is no need to provide a separate coating at the pad locations in the subassemblies made of the cold-worked material. In fact, in the French reactor Superphenix, built after Rapsodie, no hard facing or coating was provided at the contact pads. Accordingly even for Indian PFBR, it was decided to go ahead with no coating on the pad of fuel subassemblies.

1.7. Aim of the Investigation

The following are the aim of the investigation:

- To have firsthand information of the risk of self-welding in the subassemblies contact pad during the PFBR operation by conducting tests in simulated reactor conditions.
- To identify the test parameters that would result in self-welding of the mating surface for structural material and understand the mechanism of self-welding.
- To compare the self-welding susceptibility of 20% cold-worked alloy D9, the contact pad material with the structural material 316LN of PFBR.

1.8. Organisation of the thesis

The thesis is proposed to have 5 chapters:

- Chapter 1 Introduction
- Chapter 2 Scope of research
- Chapter 3 Experimental program
- Chapter 4 Results and Discussion
- Chapter 5 Conclusion

Chapter 1 briefs the features of sodium cooled Prototype Fast Breeder Reactor (PFBR) and the self-welding of mating surfaces in sodium was explained with figures. Self-welding in different components of PFBR was summarised and tabulated. The PFBR core subassemblies were discussed in detail as the focus of our study is on self-welding of contact pads of fuel subassemblies. The various options used in different reactors worldwide to prevent self-welding were discussed in detail. Finally the aim of the investigation is brought out.

Chapter 2 summarises the literature available in self-welding of mating surfaces in flowing sodium. Procedures adopted for testing by different laboratories were essentially same i.e. the specimens are pressed against each other at a known load and at a fixed temperature for a known duration. In most of the cases specimens were stacked one over the other and load was applied vertically. In some of the studies, specimens were arranged horizontally and direction of load application was horizontal. Different laboratories use different parameters to assess the susceptibility of the mating surfaces to self-welding. There is only one study reported on cold-worked austenitic stainless steel, SS316. New structural materials like 316LN and alloy D9, presently chosen for India's PFBR have not been studied for their susceptibility to self-welding.

Chapter 3 describes the experimental program carried out. It also includes the design of an experimental facility for self-welding in which parameters like load, time and material can be varied. Alloy D9 and 316LN are chosen for the experiment in annealed and cold-worked condition. 316LN is taken as reference material. The specimens are hollow rings so that they can be stacked one over other and compressed. The specimens after assembly will be inserted into a sodium vessel where sodium circulation is maintained with online purification using cold trap and plugging indicator. After the experiment, the specimen assembly is taken out and cleaned from sodium. A set up was designed to measure the shear force required for separation of the self-welded pairs. The self-welded specimen was further subjected to metallurgical studies like SEM, EDS, AES, microstructure and hardness measurement. To get the best results from the experiment, extreme care was taken throughout the experiment.

Chapter 4 discusses the results of the experiments carried out to assess the self-welding susceptibility of the material. The self-welded specimen pairs were analyzed for using self-welding coefficient, SEM, EDS, Microstructure Macro and Micro hardness. Empirical relations were derived for alloy D9 and 316LN in annealed and cold-worked condition. The SEM micrographs were presented showing the surface damage in all cases tested. The results indicated that the self-welding tendency is more in annealed 316LN than in 20% cold-worked 316LN which is on the expected line. On the contrary, 20% cold-worked alloy D9 showed more self-welding tendency and the annealed alloy D9 showed no self-welding. On analysis it was found that dynamic recrystallisation favoured self-welding tendency in 20% cold-worked alloy D9 and there was no dynamic recrystallisation in annealed alloy D9. The carburisation of alloy D9 in sodium resulted in the formation of TiC precipitates at the grain boundary near the surface which accelerated the dynamic recrystallisation in 20% cold-worked alloy D9. Thus 20% cold-worked alloy D9 was found to be more susceptible for self-welding in flowing sodium. It was also determined that for PFBR conditions, self-welding will not occur in 20% cold-worked alloy D9 contact pads of the subassemblies during its operation.

In Chapter 5 the conclusions drawn from this study are detailed along with the future directions of the self-welding studies to be carried out.

1.9 Summary

The features of sodium cooled fast reactor (PFBR) were briefed and the self-welding of mating surfaces in sodium was explained with figures. Self-welding in different components of PFBR was summarised and tabulated. The PFBR core subassemblies were discussed in detail as the focus of our study is on self-welding of contact pads of fuel subassemblies. Finally the aim of the investigation is brought out.

CHAPTER 2

SELF-WELDING SUSCEPTIBILITY STUDIES IN FLOWING SODIUM

2. SELF-WELDING SUSCEPTIBILITY STUDIES IN FLOWING SODIUM

2.1. Literature survey

Self-welding of mating surfaces of various reactor components in flowing sodium has been a concern in the design of Fast Breeder Reactors worldwide. Hence, extensive studies on self-welding susceptibility of some of the materials considered for various components of fast breeder reactors have been carried out using specially designed experimental set up for this purpose. Essence of these studies is given below:

K.Bendorf [13] of Germany in 1970 carried out experimental investigations of self-welding of structural materials in sodium as shown in Fig. 2.1. Two devices which can hold 15 and 40 specimens respectively were inserted into sodium tank and tightened by a pull rod with a bellow arrangement for leak tightness. The force is measured by annular dynamometer. Tests were conducted at two temperatures 853 K (580 ^{o}C) and 973 K (700 ^{o}C), contact stress up to 20 MPa and duration up to 7 days. Austenitic stainless steel, ferritic steel, nickel base alloy and hardfacing alloys were tested. Adhesion coefficient H, defined as

$$H = \text{Adhesive force / contact force} \qquad (1)$$

is used as a parameter to assess the susceptibility of the materials to self-welding.

It was found from the experiment that austenite and ferrite steels are susceptible to self-welding and the adhesion coefficient H is greater than unity. Repeatability of the result was found difficult due to differences in roughness, shape, mechanical and thermal influences, disassembly and cleaning of specimen.

The experimental set up was massive. Though the self-welding phenomenon is also time dependent, experiments were carried out for 7 days only. The experiments indicate that austenitic steel is susceptible for self-welding. The experiments also indicate that sodium flushing of surfaces is essential for self-welding to occur.

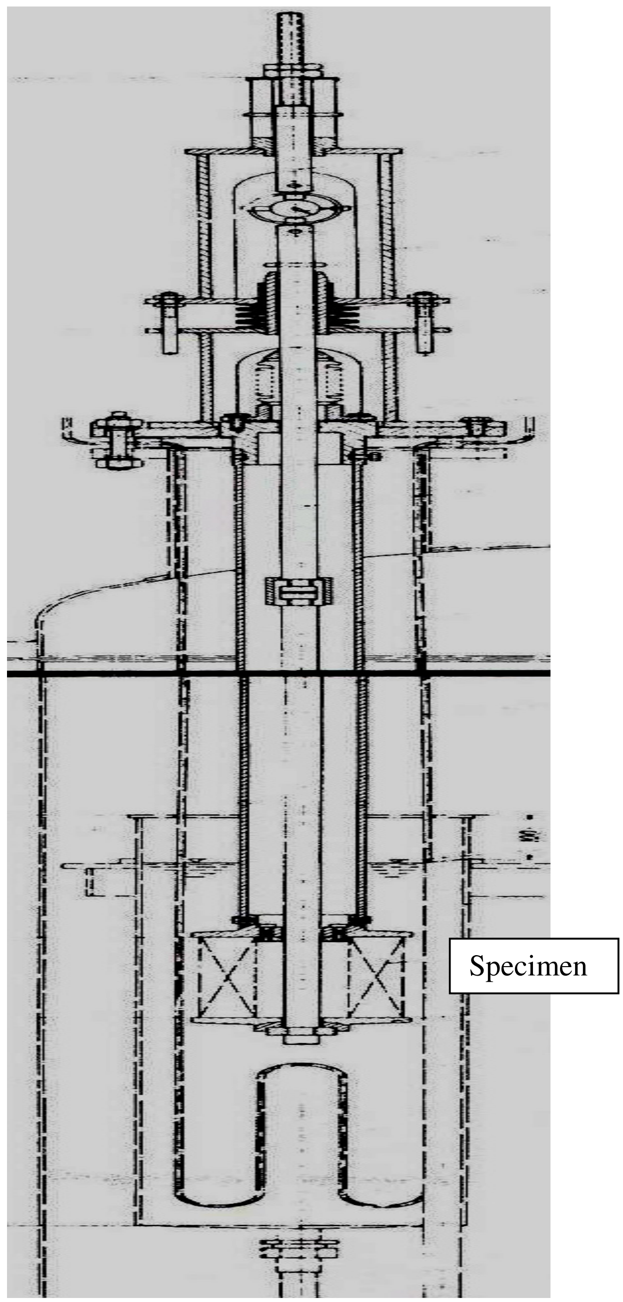

Fig. 2.1: Experimental setup of K. Bendorf [13]

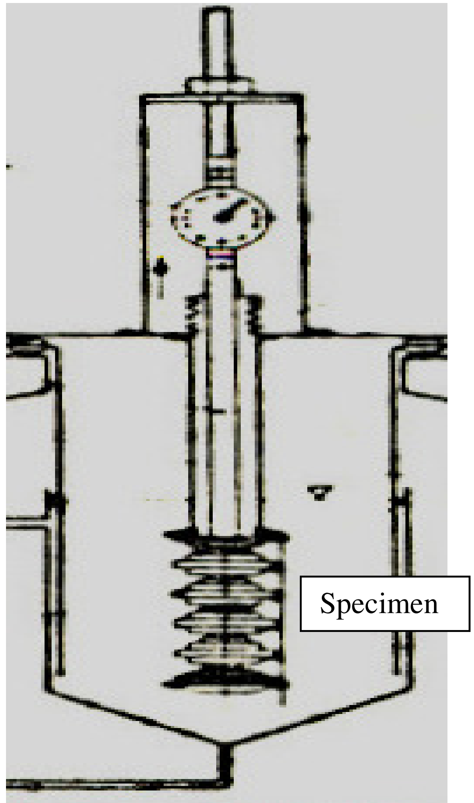

Fig. 2.2: Experimental set up of Huber [14]

Huber [14] of Germany investigated self-welding behavior of materials in sodium in the facility as shown in Fig. 2.2. The experimental set up is similar to that used by K. Bendorf. The test material and conditions were selected mainly to suit SNR 300 prototype sodium cooled fast reactor. Initial experiments were to find out the influence of material, sodium temperature, contact pressure, contact area and surface finish. Final experiments were on Inconel 718 (nickel base alloy) and stellite 6 (cobalt base alloy) for SNR 300 fuel spacer pads. It was determined from experiment that the breakaway force increased proportionally to contact area, contact pressure, and contact time. Breakaway force is inversely proportional to high temperature strength of the material. When two dissimilar materials are used, self-welding behavior is determined by material with lower high temperature strength. Maximum breakaway forces were measured with ferritic steel, lower breakaway force were obtained with austenitic steel, and lowest breakaway force was measured for inconel 718 indicating that the breakaway force is inversely proportional to high temperature strength of the material.

The test materials Inconel 718 and stellite 6 and experimental conditions were selected for the SNR 300 spacer pads. Tests were performed to evaluate more accurately the self-welding behaviour of these materials.

Ji Young [15] of United States evaluated the self-welding behavior in stellite 1, 3, 6, 12 and 21 for a range of contact stress (41.4 MPa to 82.8 MPa), sodium temperature 727 to 902 K (454 ^{o}C to 629 ^{o}C) and contact period one week to six months. One specimen is attached to the bottom of the test vessel containing sodium and other specimen is attached to a shaft through seals and hydraulic actuator. The hydraulic device is used to mate and hold the samples in static contact at the required load. Stellite 1, 6, 12 were hardfaced on 304 stainless steel by oxy-acetylene deposition process and plasma transfer arc process was used for Stellite 21. Stellite 3 was tested in as cast condition. The thickness of coating was maintained greater than 3.2 mm in order to minimize dilution of coating by base material. It was found from the experiment that:

$$\text{Breakaway force} = A\, t^{1/2} \qquad (2)$$

where t is the time of contact and A is proportional constant which is function of sodium temperature, material, surface morphology and contact stress.

The figure of the experimental set up is not provided. The paper deals with stellite series under cyclic loading conditions. Stellite 1 showed superior self-welding resistance compared to other material because of higher carbon content in the alloy.

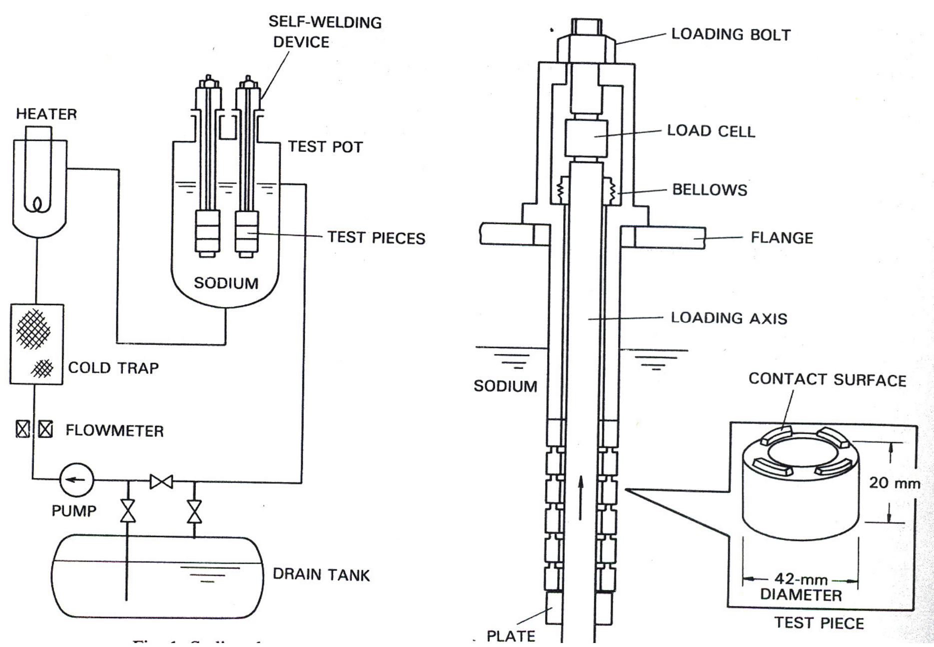

Fig. 2.3: Experimental set up of Norikatsu [16]

Norikatsu [16] of Japan in 1986 studied the self-welding of FBR structural materials (type 304, type 321, inconel 718, and 2.25 Cr -1Mo steel) in sodium using the facility as shown in Fig. 2.3 up to a contact pressure of 98 MPa for 100 to 900 h at temperatures ranging from 778 K to 823 K (505 ^{o}C to 550 ^{o}C). The experimental set up consists of a load cell, loading bolt and specimens, inserted from the top of the vessel with bellows for leak tightness. The bottom face of the specimen had curved ridges for which lengths are varied to get the desired contact pressure. Self-welding coefficient, W was defined as breakaway force per unit contact force. It was found that the self-welding coefficient W is proportional to square root of contact time and increased with increase in temperature of sodium.

$$W^2 = K\,t \qquad (3)$$

where W = self-welding coefficient K = rate constant of self-welding

t = contact time.

Type 304, Type 321, and Inconel 718 materials had almost same value of self-welding coefficient. 2.25 Cr-1Mo steel self-welded to itself and susceptibility to self-welding was highest among the material combinations studied. It was also found that at the interface of self-welding, chromium is rich and it forms a barrier for diffusion of atoms. Presence of chromium was attributed as one of the reasons for better self-welding resistance of stainless steel than 2.25Cr 1Mo steel.

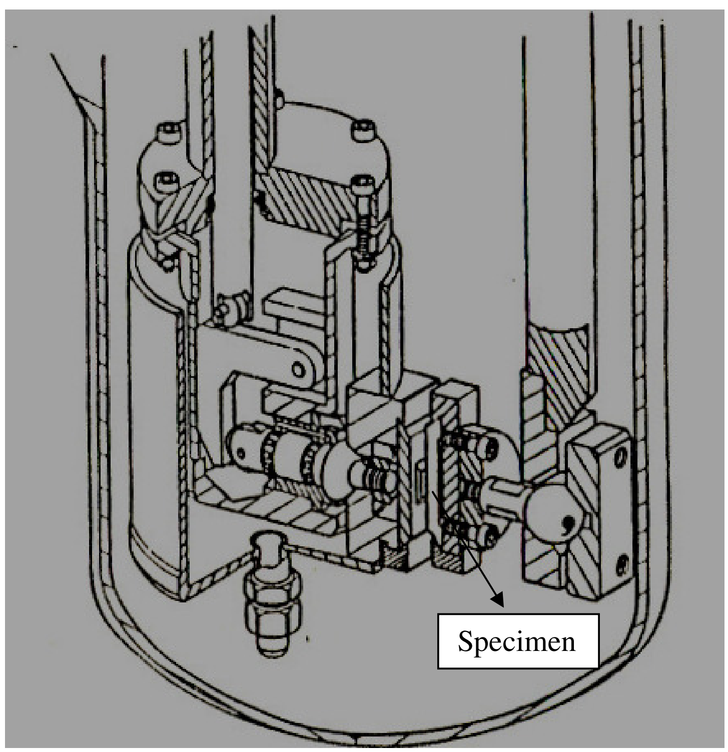

Fig. 2.4: Experimental set up of P.Agostini [17]

Agostini [17] of Italy have carried out self-welding tests in sodium in the facility as shown in Fig. 2.4, at 673 K and 773 K (400 ^{o}C and 500

^{o}C) on 20% cold-worked SS 316 up to a maximum of 45 days. A contact force of 530 N was applied.

The specimens had a flat to flat contact and were tested in static condition in a reciprocating tribometer used for friction measurement. 20% cold-worked 316 was tested up to 45 days. It was concluded that no self-welding had occurred.

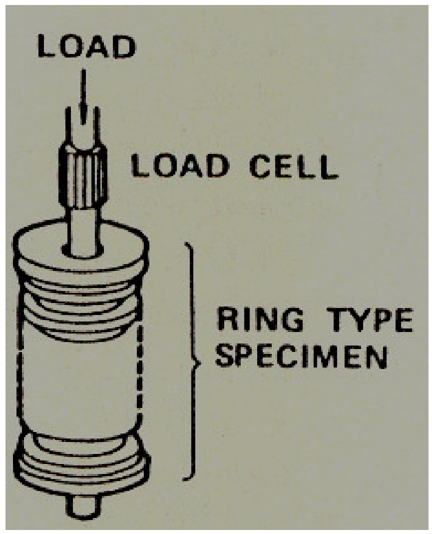

Fig. 2.5: Experimental set up of Yoshida [18]

Yoshida [18] of Japan has carried out in-sodium tribological study, which includes self-welding test in a set up as shown in Fig. 2.5, on cobalt-free hard facing materials chosen to reduce the radiation exposure in FBR. The test specimens were stacked together, inserted into the pull rod and exposed in sodium. Nickel base alloys Fukudalloy 453, Comonoy-6, Metco 15E and Triboloy 700 were tested with contact stress up to 40 MPa for duration up to 3200 hours.

Graphs were plotted between self-welding ratio (number of self-welded specimen / number of test specimen) and sodium temperature with SS 316 and Stellite 6 as reference materials. At temperatures above 873 K (600 ^{o}C) all specimens showed self-welding.

Sulekh [4] of India investigated self-welding in combinations of austenitic stainless steel (Fig. 2.6 and Fig. 2.7), hard chrome plating and stellite-6 in liquid sodium at 803 K (530 ^{o}C) with contact pressure 10 and 40 MPa for 500 h and 1000 h. The test specimens were stacked in a rod and pressed against the sodium vessel at its bottom. The applied force was calculated by deflection and stiffness of the spring used in the test set up. There were indications of mild self-welding in all combinations of material tested except stellite combinations.

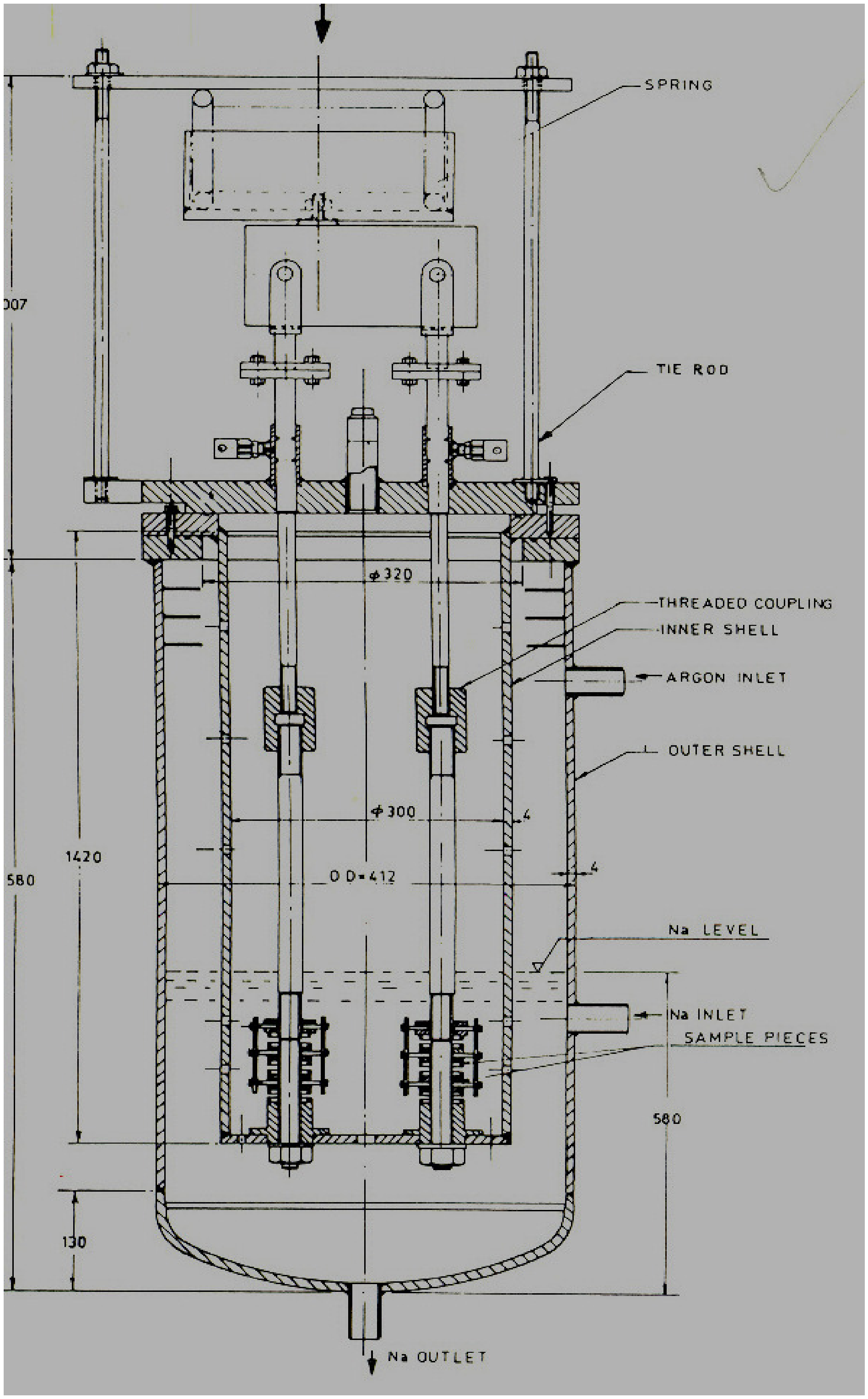

Fig. 2.6: Experimental set up of Sulekh Chander [4]

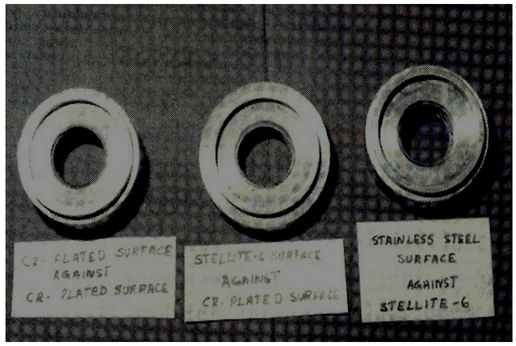

Fig. 2.7: Specimen used by Sulekh [4]

Hemant [19] of India has qualified chromium plated 2.25Cr -1Mo steel and Inconel 82 for PFBR as no self-welding was observed during the simulated test conditions. This material combination is used in Diverse Safety Rod Drive Mechanism (DSRDM). Experiment was carried out at 823 K for 3 months under contact stress of 9.4 MPa.

From the survey of the literature reported on self-welding susceptibility studies in flowing sodium, it can be seen that several material combinations which are relevant to FBRs have been studied by different laboratories in many countries. In general, hardfacing coatings and high temperature Ni base alloys have exhibited better resistance to self-welding than the structural materials like austenitic stainless steel and 2.25Cr-1Mo steel. There is only one study reported on cold-worked austenitic stainless steel, SS316. New structural materials like 316LN and alloy D9, presently chosen for India's PFBR have not been studied for their susceptibility to self-welding.

Procedures adopted for testing by different laboratories were essentially same i.e. the specimens are pressed against each other at a known load and at a fixed temperature for a known duration. In most of the cases specimens were stacked one over the other and load was applied vertically. In some of the studies, specimens were arranged horizontally and direction of load application was horizontal.

Different laboratories use different parameters to assess the susceptibility of the mating surfaces to self-welding. Bendorf [13] defined Adhesion Coefficient, H as a parameter to assess self-welding susceptibility. Ji Young [18] considered breakaway force of the self-welded specimen for the same purpose. Norikatsu [16] used self-welding coefficient W, defined as ratio of breakaway force to contact force as the parameter. Yoshida [18] chose self-welding ratio, which is the ratio of number of specimens self-welded to number of specimens tested as the parameter. A close look at these parameters reveals that parameter, H breakaway force and parameter, W is closely related. However, the parameter W normalizes the breakaway force with contact force and is found to increase with duration of the test according to the Eqn. 3 ($W^2 = K\ t$). This makes it suitable for independent verification.

2.2. Scope of research work

Reactor core is a critical part which is subjected to extreme conditions of high temperature, liquid sodium and nuclear radiation in FBRs. To achieve compactness in core the fuel subassemblies are hexagonal in shape and pads are provided in all the six faces of hexagon to maintain uniform clearance. Alloy D9, which has higher void swelling resistance and irradiation creep resistance than 316LN, the major structural material for PFBR, was specially developed and tested as material for subassemblies contact pads[10,11]. As cold-work further improves resistance to radiation swelling, alloy D9 is 20% cold-worked. Literature survey revealed that no data is reported on self-welding of 20% cold-worked alloy D9. Hence, an experimental program was planned to study self-welding susceptibility of alloy D9 both in cold-worked and annealed conditions in flowing sodium and compare the results with those obtained for similar studies carried out on 316LN, the major structural material of PFBR.

The major objective of this study is to find out if self-welding will occur between the contact pads of adjacent fuel subassemblies during reactor operation. Hence an accelerated test was conducted using 20% cold-worked alloy D9 specimens in flowing sodium simulating reactor conditions. Eqn. 3 ($W = K\, t^{1/2}$) was used to determine the contact stress for 3 months under accelerated test conditions. Later in the experiment, the contact stress and duration were varied to study the self-welding behavior of alloy D9 and 316LN steel.

The research work starts with literature survey. Based on the objective, alloy D9 and 316LN are selected for the experimental study. Identification of alloy D9 and 316LN rods in annealed condition and 20% cold-working of a part of the rods. Machining the specimens from annealed and cold-worked condition for the experiment are also in the scope of research work. This also includes polishing of specimens and measuring the surface finish to the required level. All safety precautions are to be taken care during the operation of the sodium loop for the experiment due to high temperature and sodium is a highly reactive coolant. Results obtained from these tests also need to be reliable and accurate. Design of such a test facility should be such that handling of specimens for testing, cleaning and dismantling are easy. Hence, design and fabrication of an experimental facility for self-welding in which parameters like load, time and material can be varied form part of the scope of this work. Similarly design and fabrication of the set up to measure the breakaway force to separate the self-welded specimen is also forms part of this work. Finally, metallurgical characterization of the material both before and after the self-welding susceptibility tests was also covered under this research work.

2.3 Summary

All the experiments carried out worldwide for self-welding susceptibility in flowing sodium were studied. These studies were carried out in Germany, USA, Japan and Italy. In general, hardfacing coatings and high temperature Ni base alloys have exhibited better resistance to self-welding than the structural materials like austenitic stainless steel. There is only one study reported on cold-worked austenitic stainless steel, SS316. New structural materials like 316LN and alloy D9, presently chosen for India's PFBR have not been studied for their susceptibility to self-welding. In most of the cases specimens were stacked one over the other and load was applied vertically. In some of the studies, specimens were arranged horizontally and direction of load application was horizontal.

Bendorf [13] defined Adhesion Coefficient, H as a parameter to assess self-welding susceptibility. Ji Young [18] considered breakaway force of the self-welded specimen for the same purpose. Norikatsu [16] used self-welding coefficient W, defined as ratio of breakaway force to contact force as the parameter. Yoshida [18] chose self-welding ratio, which is the ratio of number of specimens self-welded to number of specimens tested as the parameter. A closer look reveals, H breakaway force and W the self-welding coefficient are closely related. However, the self-welding coefficient W normalizes the breakaway force with contact force and is found to increase with duration of the test according to the Eqn. 3 ($W^2 = K t$).

The major objective of this study is to find out whether self-welding can occur between the contact pads of adjacent fuel subassemblies during reactor operation. Hence an accelerated test was conducted using 20% cold-worked alloy D9 specimens in flowing sodium simulating reactor conditions. Eqn. 3 ($W= K t^{1/2}$) was used to determine the contact stress for 3 months under accelerated test conditions. Later in the experiment, the contact stress and duration were varied to study the self-welding behavior of alloy D9 and 316LN steel

CHAPTER 3

EXPERIMENTAL

PROGRAM

3. EXPERIMENTAL PROGRAM

3.1 Experimental Plan

3.1.1 Introduction

The experiment involves identification of alloy D9 and 316LN material, specimen preparation, design of experimental set up, introduce into a sodium system with high temperature flowing sodium, cleaning the sodium after the experiment, measurement of shear force of separation of the self-welded pairs by designing a set up, and metallurgical studies on the tested specimens. The experimental set up is planned such that 5 pairs of specimen under self-welding susceptibility study can be assembled outside and inserted into a vessel with flowing sodium. The loading of the specimen is to be done from outside and maintained during the experiment. The sodium purity is also to be maintained throughout the experiment. Alloy D9 and 316LN are chosen for the study in annealed and cold-worked condition. 316LN is taken as reference material for comparison of results.

3.1.2 Material Chemistry

The chemical composition of alloy D9 and 316LN austenitic stainless steel is shown in Table 3.1. The alloy D9 and 316LN is received in solution annealed condition, in which the material is heated to 1323 K for 30 minutes and cooled to room temperature in still air. Part of alloy D9 and 316LN are subjected to cold-work by reducing the area of cross section of the rod by 20% in tensile testing machine. The cold-worked specimens for testing are machined from these rods.

Table 3.1: Chemical compositions of alloy D9 and 316LN (wt %) [10]

Material	Ni	Cr	Mo	Mn	Si	Ti	C	P	S	N	Fe
Alloy D9	15.07	15.05	2.25	1.51	0.51	0.32	0.05	0.01	0.0025	66 ppm	Bal*
SS 316LN	12	17	2.3	1.6	0.5	0.05	0.03	0.03	0.01	0.06	Bal*

Bal*- Balance

3.1.3. Test facility

The test facility used for self-welding studies by Sulekh [4] in our research centre had the following limitations with respect to the requirements of this study.

- The loading system is bulky and handling is not easy.
- The compression load is not accurately measurable
- After the experiment, removal of the self-welded specimen pairs (without breaking) from the test set up was difficult.
- The specimens were bulky and hence compressive force has to be applied in tonnes.
- O-rings in the nozzles get damaged and leaking during the assembly of the specimen and leak tightness is a problem.
- No arrangement was there to measure breakaway force of self-welded specimen after the test.

All these drawbacks were overcome in my new design used for the study so that handling is simple and easy as shown in Fig. 3.1 [20]. The vessel is fully welded type with four number of one inch pipe nozzles with flanged end. Load cell with electronic indicator is used to know the compressive load. Load is applied with Belleville disc spring. Specimen can be assembled and inserted into sodium test vessel. At a time, four sets of specimens can be tested in parallel and independently. The contact stress is increased by reducing the contact area in the cylindrical ring by introducing a step at one side of the specimen. The specimens are small and can be easily inserted in one inch pipe nozzle. Maximum load applied is only 200 kg. After experiment, removal of specimen from test set up is easy and self-welded pair remained intact. Thermocouples are fixed in the vessel and fully insulated. Sodium level is indicated by level probes and argon is used as cover gas above the free sodium level. Initially 1 to 2 mm gap is maintained between specimens for sodium to remove the oxides for one day. Then specimens were compressed by Belleville spring. A load cell is attached to indicate the compression load. Five specimens are stacked at a time. The specimens are machined from alloy D9 and 316LN rods in annealed and 20% cold-worked condition as shown in Fig. 3.2 (a). The OD is 21.4 mm; ID is 15.8 mm and 15 mm height. In some specimen a step is machined on one side (18.8 mm dia and 1.5 mm depth) to increase the contact stress at the mating surfaces for the same spring load applied at the top. The mating surfaces were polished for a surface finish less than 0.5 μm. The roughness average of the surface of the specimen was checked with Surface Roughness Tester (Mitutoyo SJ-201). Two holes are drilled on the side to facilitate the measurement of the shear force required to separate the self-welded pairs. The specimen identification mark is engraved on the surface of each specimen. The specimen assembly is shown in Fig. 3.2 (b). The specimens under study are assembled and the sequence of stacking are recorded before inserting into the test vessel. After fixing the specimen assembly in the test vessel, leak tightness is checked by pressuring the sodium vessel with argon. Then the experiment is conducted as scheduled.

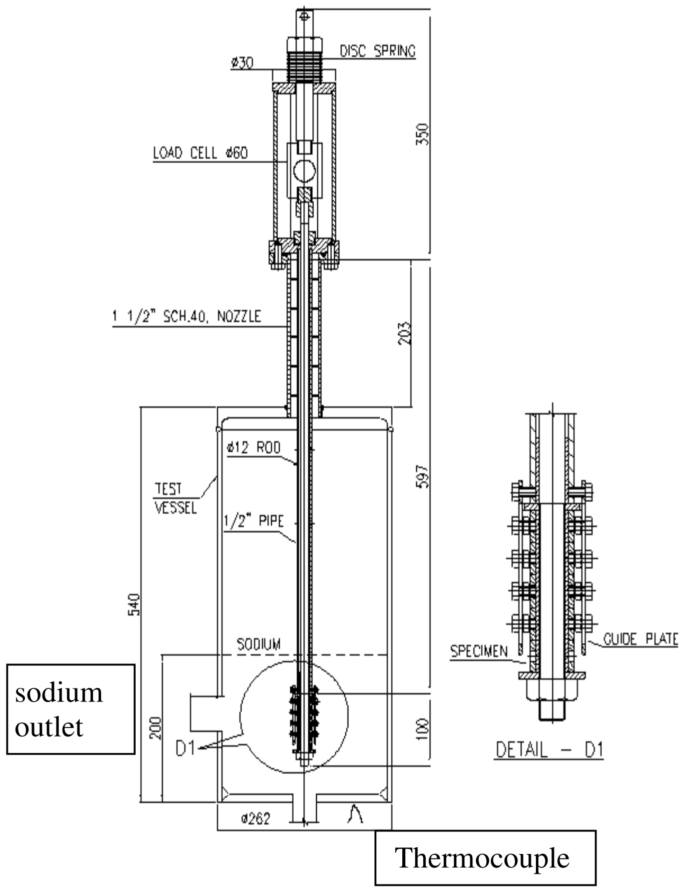

Fig. 3.1: Assembly of specimen in sodium vessel [20]

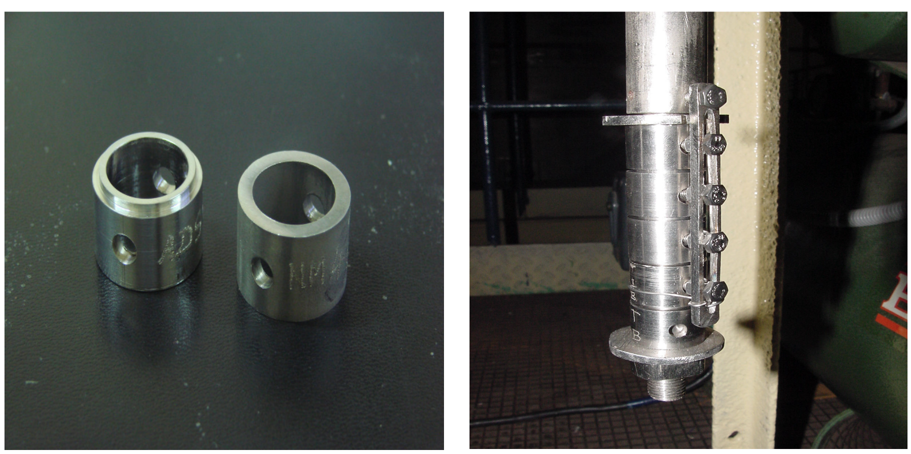

(a) (b)

Fig. 3.2: Specimens for self-welding tests [20]

3.1.4. Set up for shear force measurement of self-welded specimen

After the completion of the test, the specimen assembly is taken out from the test vessel, cooled to room temperature and cleaned from sodium using alcohol. The contact load is removed in the specimen assembly by loosening the Belleville disc spring and the self-welded pair is indentified and taken out carefully. The self-welded pair is separated by application of shear force. The set up designed for this purpose is as shown in Fig. 3.3 [21]. It consists of a mechanical vice to hold one of the self-welded specimens. Belleville spring is used to give shear force perpendicular to the axis of the specimen by gradual tightening of nut at the other end. A load cell is used to monitor the applied force. The other specimen is held in a split pipe and gripped by vice to avoid bending force.

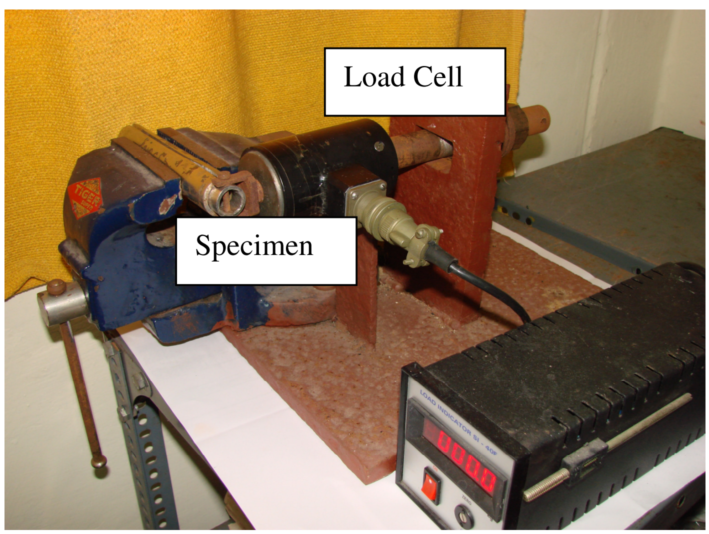

Fig. 3.3: Set up for breakaway force measurement [21]

3.1.5. Sodium Loop

The sodium loop used in this investigation is shown in Fig. 3.4. Sodium is heated to 473 K in storage tank and then it is filled in the loop. The electromagnetic pump circulates sodium through heater vessel and a small flow of about 20% through plugging indicator and cold trap.

Sodium is heated by heater vessel. The plugging indicator indicates sodium purity level and cold trap purifies sodium continuously. The mixed sodium flow is adjusted such that the sodium entering the test vessel is at 823 K and returned to storage tank from where the sodium is sucked back to the loop by electromagnetic pump. The sodium used in the loop is 99.95% pure (Reactor grade purity). Argon is used as cover gas in the vessel above the sodium level. Sodium picks up moisture from argon cover gas during the assembly of the experimental set up to form oxides and hydrides. These impurities can be removed from sodium by cold trap and maintained below 2 ppm (cold point of sodium maintained at 388 K in the cold trap). Carbon present in sodium is about 25 ppm. When the loop is not in use, sodium is dumped to storage tank and cooled to room temperature. Fig. 3.5 shows the specimen in assembled condition and Fig. 3.6 shows the test vessel and other accessories of sodium loop.

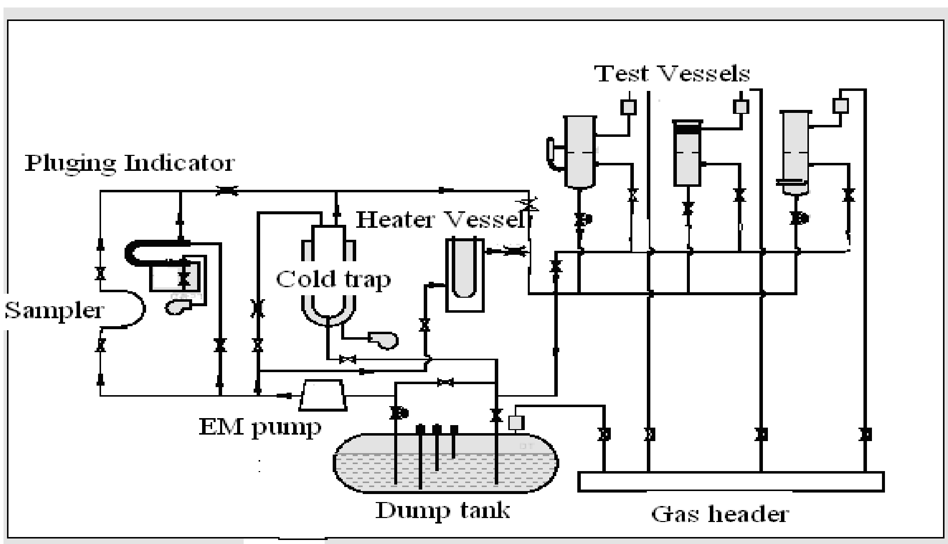

Fig. 3.4: A typical sodium loop [22]

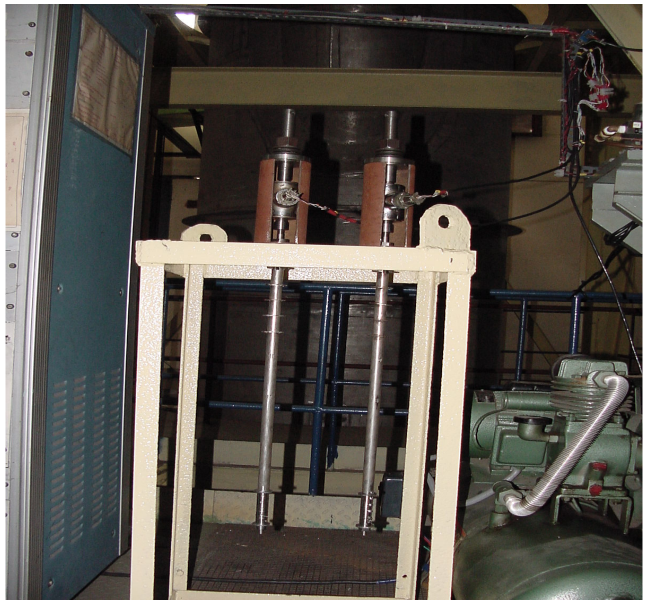

Fig. 3.5: Specimen assembly before insertion in sodium vessel.

Fig. 3.6: Sodium loop used for self-welding studies

3.2 Experimental Program

3.2.1 Accelerated test for PFBR

It is important to ensure that self-welding between the subassemblies made of 20% cold-worked alloy D9 do not take place during reactor operation in PFBR. Accelerated tests were carried out for 3 months and the load level corresponding to the tests of 3 month duration were estimated using the equation 3 ($W = K\ t^{1/2}$) obtained from literature survey [16] where 'W' is the self-welding coefficient, 'K' is a constant and 't' is the duration of test. Self-welding coefficient is defined as the shear stress for breakaway per unit contact stress (shear force / contact force) and is used to compare the self-welding susceptibility of various combination of material. Hence instead of testing with contact stress of 3.3 MPa for 24 months as required in PFBR (Table 1.1), test time is fixed as 3 months and the contact stress for accelerated test is calculated as given below.

$$W_{24} = K\ t_{24}^{\ 1/2} \qquad (4)$$

$$W_3 = K\ t_3^{\ 1/2} \qquad (5)$$

where W_{24} is the self-welding coefficient for 24 months (t_{24}) and W_3 is the self-welding coefficient for 3 months (t_3) and K is the constant. Dividing equations 4 by equation 5, the ratio of W_{24} to W_3 is 2.8. Assuming that self-welding take place and breakaway shear stress would be same for both durations, and then the ratio of contact stress for 3 months and 24 months becomes 2.8. Hence the contact stress for 3 months is estimated as (3.3 x 2.8) 9.4 MPa. Hence the experiments started with 20% cold-worked alloy D9 specimen with contact stress of 9.4 MPa for 3 months. If self-welding does not occur after the test conducted at these test parameters, it can be concluded that the contact pads are unlikely to be self-welded during the service in PFBR. Later the contact stress is increased up to 24.5 MPa and duration up to 9 months to study the mechanism of self-welding in alloy D9 and 316LN in annealed and 20% cold-worked condition in more detail.

3.2.2 Overall Experimental conditions maintained

The following are the experimental conditions:

Sodium temperature	823 K
Oxide and hydrides impurities	< 2 ppm
Carbon impurity	< 25 ppm
Contact Stress	9.4 MPa to 24.5 MPa
Duration	3 or 4.5 or 6 months or 9 months
Surface finish	< 0.5 µm
Material tested	1) annealed and 20% CW alloy D9
	2) Annealed and 20% CW 316LN

The tests were carried out round the clock without interruption for specific duration. The experimental conditions were recorded every day and the contact stress is maintained constantly by the load cell and disc spring. The sodium is purified by cold trap continuously, a component in sodium loop which removes the oxide and hydride impurities of sodium due to surface adhesion by lowering the sodium temperature.

3.2.3 Experiment carried out

The sodium loop and test vessel were preheated to 573 K (300 ^{o}C). Sodium is filled in the test vessel at 473 K. The sodium level is indicated by level probe. It is ensured that the specimens were immersed in sodium. Part of the test vessel above the sodium level is maintained under argon atmosphere at a pressure higher than the atmosphere. With additional surface heater provided in the vessel the sodium temperature could be raised to 823 K during the experiment.

When the specimens were assembled in the test vessel, 1 to 2 mm gap is provided between the specimens. This will help in free flow of sodium over the mating surfaces. The pure sodium (reactor grade) removes the oxide layer over the mating surface and exposes clean metal. On loading the specimen after 24 hours, metal to metal contact takes place and sodium temperature is raised to 823 K and specimen assembly is loaded to the predetermined load so that the mating surfaces are in contact at the desired stress level.

A load cell connected to the mechanism indicates the load applied. The load is set for pre-determined contact stress in the experiment based on the area of contact. The load cell also indicates the load during the experiment and periodically the load is checked and corrected for any variation. Fig. 3.7 shows the control room and Fig. 3.8 and 3.9 show the specimen being inserted in the test vessel for fixing.

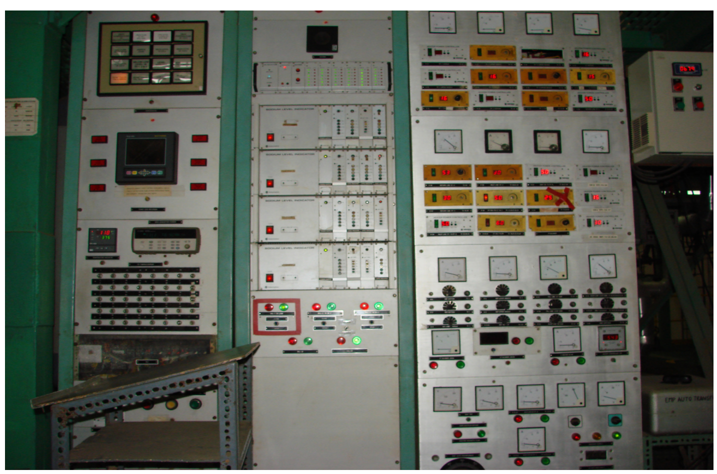

Fig. 3.7: Control Room for self-welding studies

3.2.4. Cleaning of specimens

After the completion of experiment the sodium temperature is reduced to 473 K and dumped in storage tank. The test vessel is cooled to room temperature and specimen assembly was taken out. Figure 3.10 shows the specimen with sodium deposit. Sodium is cleaned using alcohol. The specimen assembly is dipped in an alcohol container.

Fig. 3.8: Specimen assembly inserted in sodium test vessel

Fig. 3.9: Sodium test vessel with specimen assembly

The sodium reacts with alcohol raising the alcohol temperature. The alcohol temperature is to be controlled to room temperature to avoid catching fire. Figure 3.11 shows the sodium cleaning process. After all the sodium has reacted with alcohol the loading is released and specimens are taken out carefully to avoid break in self-weld developed in the experiment. Finally specimens are cleaned in water and dried. Figure 3.12 shows the specimens after testing and removing of sodium.

3.2.5 Measurement the shear force

If the specimens are self-welded after the test, they are separated by measuring the shear force using the experimental set up shown in Fig. 3.3 where one of the self-welded pair is held in the mechanical vice and other is connected to load cell and bolt nut mechanism. As the nut is tightened, the shear force applied is noted from the indicator. The shear force applied to the self-welded specimen pair is gradually increased till the specimens are separated and the load at which this occurs is noted as shear force to break the self-welding of the specimen pair. It should be noted that the specimen pair are taken out from sodium vessel removing all loadings, cooled to room temperature, cleaned from sodium and then only shear force measurement is made. Care is taken to avoid any bending force during separation of self-welded pair.

Fig. 3.10: Specimen assembly with sodium deposits after taking out from the vessel

Fig. 3.11: Specimen inserted in alcohol vessel to remove sodium

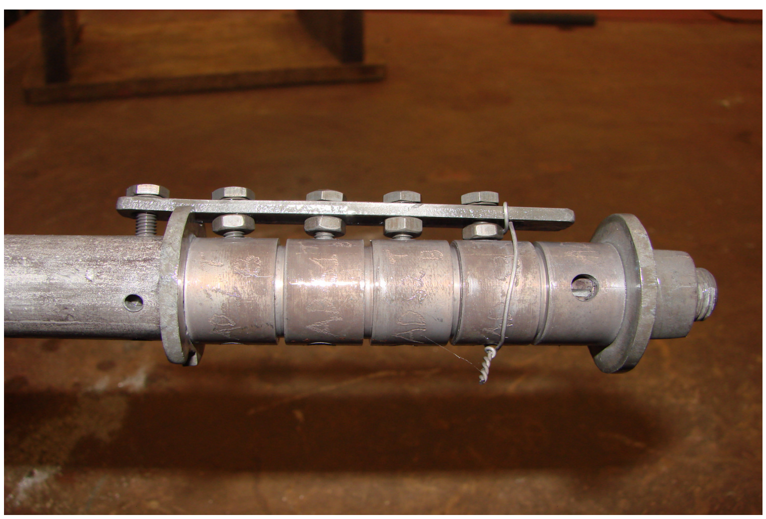

Fig. 3.12: Specimen cleaned from sodium ready for dismantling

3.2.6 Care for safety and accuracy

To get the best results from the experiment, extreme care is taken throughout the experiment. The dimensions were checked after machining for each of the specimens and noted. The mating surfaces of the specimens were polished (abrading under water using progressively finer silicon carbide paper) to ensure surface roughness is uniform and maintained below 0.5 µm. The load cell and its indicator of the test vessel were calibrated against known load. Similarly the load cell and indicator used for shear force measurement of self-welded pairs were also calibrated. The nozzles of the test vessel were numbered and record of specimen assembly in each nozzle along with its test conditions is noted. The oxide impurity in sodium is maintained below 2 ppm throughout the experiment by cold trapping (cold point maintained at 388 K). The sodium temperature is controlled to 823 ±1K.

3.2.7 *Examinations carried out*

The surface of the self-welded specimens were examined by Scanning Electron Microscope (SEM) and various elements present on surface were identified using Energy Dispersive X-ray Spectroscopy (EDS) attached with the SEM. Microstructure and hardness of the specimens after testing were compared with those before the testing. Auger electron spectroscopy (AES) is carried out on selected surface to check for carburization of the specimens from flowing sodium during the test. A small piece is cut from the specimen as shown in Fig. 3.13 for metallographic analysis. The line AB represents the thickness of the specimen. Points C and D represent the point of contact with adjacent specimen and E is not experiencing any contact stress because of step provided in the specimen. Micro hardness profile was taken at location C, D and E marked in the cut specimen along the length of the specimen perpendicular to AB.

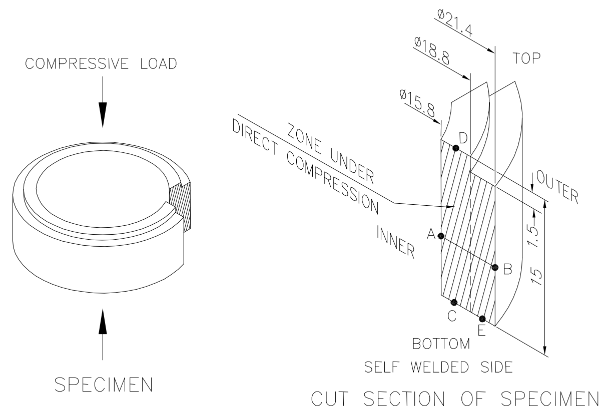

Fig. 3.13: Cut section of self-welded 20% cold-worked specimen for metallographic analysis

3.3 Summary

Alloy D9 and 316LN are chosen for the experiment in annealed and cold-worked condition. 316LN is taken as reference material. The specimens are hollow rings so that they can be stacked one over other and compressed. The specimens after assembly will be inserted into a sodium vessel where sodium circulation is maintained with online purification using cold trap and plugging indicator. After the experiment, the specimen assembly is taken out and cleaned from sodium. A set up was designed to measure the shear force required for separation of the self-welded pairs. The self-welded specimen was further subjected to metallurgical studies like SEM, EDS, AES, microstructure and hardness measurement. To get the best results from the experiment, extreme care was taken throughout the experiment.

CHAPTER 4

RESULTS & DISCUSSIONS

4. RESULTS AND DISCUSSION

4.1. Microstructure and hardness of the materials tested

Microstructure of the specimens before testing was recorded after electrolytically etching the specimens using 10% oxalic acid. The micrographs of the specimens are shown in Fig. 4.1. Hardness measurements of these specimens were carried out using Vickers hardness tester and the results are listed in Table 4.1. There is a clear difference in the microstructure and hardness between the annealed and cold-worked samples. Twin density is substantially high after cold-work. Hardness increases by more than 100 VHN (Vickers Hardness Number) in both the steels after 20% cold-work.

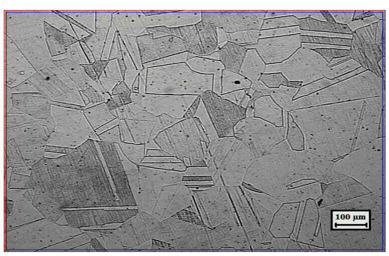

Annealed 316LN

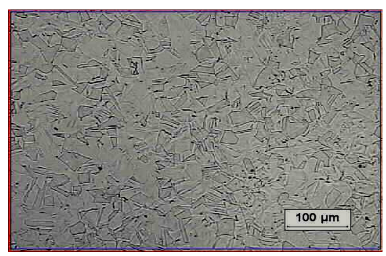

20%Cold-worked 316LN

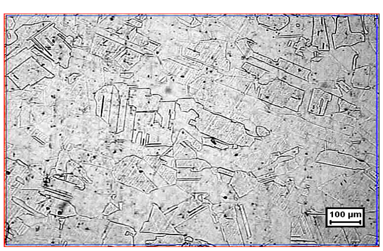

Annealed D9

20% Cold-worked alloy D9

Fig. 4.1: Microstructure specimens before self-welding susceptibility studies in flowing sodium at 823 K

Table 4.1: Bulk Hardness (VHN) before self-welding tests

Material	Hardness (VHN)
Annealed D9	134±1
20%cold-worked D9	238±1
Annealed 316LN	145±1
20%cold-worked 316LN	265±1

4.2. Self-welding susceptibility results

The accelerated test for self-welding susceptibility of PFBR contact pad indicated no self-welding in the 20% cold-worked alloy D9 specimens tested with 9.4 MPa contact stress for 3 months in flowing sodium at 823 K. Hence it can be concluded that self-welding will not take place in the contact pads of fuel subassemblies of PFBR. To study self-welding susceptibility further in 20% cold-worked alloy D9, tests were continued for 6 months at 9.4 MPa and 9 months with increased contact stress of 12 MPa. Results showed that self-welding has occurred in 6 and 9 months tests of 20% cold-worked alloy D9. One test is conducted in 20% cold-worked alloy D9 with a contact of 24.5 MPa and duration of 4.5 months and self-welding is observed in this test also. From the results, it can be concluded that self-welding takes place in 20% cold-worked alloy D9 under prolonged duration or at higher contact stress. The number of pairs self-welded in each test for cold-worked alloy D9 and their breakaway forces are shown in Table 4.2.

Table 4.2: Results of self-welding tests of alloy D9 in sodium at 823 K

Material Combination	Dwell Time *t* (months)	Contact force (N)	Contact area (mm^2)	Contact pressure (MPa)	Self-welding behaviour	No. of pairs tested	No. of pairs self-welded	shear force (N)	Self-welding coefficient (shear force/ contact force)W	$t^{1/2}$
20%CW* D9 and 20%CW* D9	3 (2160 h)	1566	166.5	9.4	No self-welding	2	Nil	0	0	46.4
20%CW* D9 and 20%CW* D9	4.5 (3240 h)	2000	81.6	24.5	Self-welded	3	1	182	0.1	56.9
20%CW* D9 and 20%CW* D9	6 (4320 h)	1566	166.5	9.4	Self-welded	2	1	202	0.13	65.7
20%CW* D9 and 20%CW* D9	9 (6480 h)	2000	166.5	12	Self-welded	4	2	330, 252	0.16, 0.13	80.5
Annealed D9 and annealed D9	3 (2160 h)	1566	166.5	9.4	No Self-welding	1	Nil	0	0	46.4
Annealed D9 and annealed D9	4.5 (3240 h)	2000	81.6	24.5	No Self-welding	3	Nil	0	0	56.9
Annealed D9 and annealed D9	6 (4320 h)	1566	166.5	9.4	No Self-welding	1	Nil	0	0	65.7

CW*-cold-worked

Table 4.3: Results of self-welding tests of 316LN in sodium at 823 K

Material Combination	Dwell Time *t* (months)	Contact force (N)	Contact area (mm^2)	Contact pressure (MPa)	Self-welding behaviour	No. of pairs tested	No. of pairs self-welded	shear force (N)	Self-welding coefficient *W* (shear/ contact force)	$t^{1/2}$
20%CW* 316LN and 20%CW* 316LN	3 (2160 h)	2000	81.6	24.5	Self-welded	3	1	117	0.06	46.4
20%CW* 316LN and 20%CW* 316LN	4.5 (3240 h)	2000	81.6	24.5	Self-welded	4	1	160	0.08	56.9
Annealed 316LN and annealed 316LN	3 (2160 h)	2000	166.5	12	Self-welded	4	3	382, 382, 637	0.19, 0.19, 0.32	46.4

CW*-cold-worked

Table 4.2 also contains results of the tests conducted for annealed alloy D9. In contrast to what is observed for cold-worked alloy, annealed alloy D9 exhibited remarkable resistance to self-welding. Specimens prepared from the annealed alloy D9 were also tested for 3 months at 9.4 MPa, 4.5 months at 24.5 MPa and 6 months at 9.4 MPa similar to the tests conducted for 20% cold-worked alloy D9. Results indicate that no self-welding has taken place. Hence it is concluded that annealed alloy D9 is resistant to self-welding.

Four pair of annealed 316LN specimens were subjected to 12 MPa contact pressure for a period of 3 months in flowing sodium at 823 K. It was found that 3 pairs got self-welded. The results were in line with that of annealed 304 and 321 reported by Yokota [16]. 20% cold-worked 316LN specimens tested for 3 months and 4.5 months at contact pressure of 24.5 MPa in flowing sodium at 823 K also got self-welded. The results are shown in Table 4.3.

On examinations of the test specimens it is found that self-welding occurred only on few locations on the surface and not over the entire mating surface. Hence the actual contact area will be less as the specimens were in contact only in the asperities of the mating surface. However for comparing with different combinations of testing, the contact stress in the experiment is estimated assuming 100% contact between the two mating surfaces.

Though the specimens of same material combinations were tested under same experimental conditions, all the pairs did not self-weld equally. This is due to variations in the actual contact area at the asperities of the mating surfaces of the specimens during loading. The pair with relatively minimum contact area at the asperities of the mating surfaces experiences high contact stress gets self-welded easily.

4.3. Variation of self-welding coefficient with time

The linear relation between self-welding coefficient and square root of the duration of test is first reported by Yokata [16] and results of our tests carried out using annealed and cold-worked 316LN and alloy D9 also confirm validity of this relation as shown in Fig. 4.2. The results reported for annealed 304/321 by Yukota [16] and annealed 316LN from the present study fall in the same line in the figure. Hence it is believed that annealed 304/321/316LN have similar self-welding susceptibility in high temperature sodium. Similarly the experimental data for 20% cold-worked D9 and 20% cold-worked 316LN also follow the linear relation between self-welding coefficient and square root of the duration of test. Hence it can be stated that the linear relationship proposed by Yukota is valid even for cold-worked material. It is also noted that annealed 316LN shows least resistance to self-welding and annealed alloy D9 do not self-weld in the range of stress levels and durations studied. However, cold-working makes alloy D9 susceptible to self-welding and under same test conditions. In contrast, cold-working seems to reduce the susceptibility of 316LN to self-welding in flowing sodium.

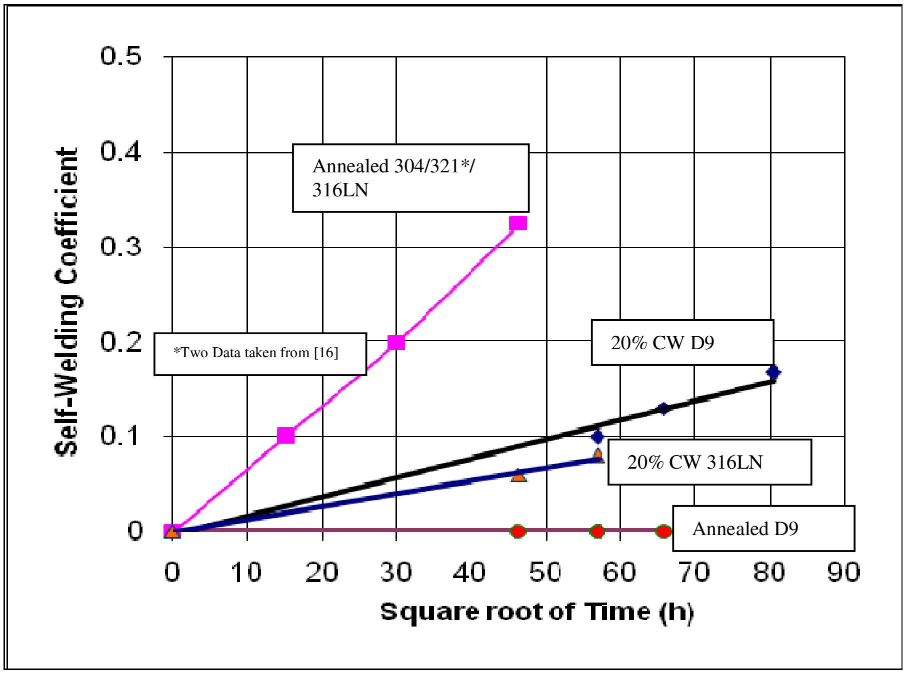

Fig. 4.2: Self-welding susceptibility of D9 and 316LN sodium at 823 K

Increase in breakaway force of self-welded specimens with increase in duration of testing can be explained as follows. Initially, the actual contact area at the asperities (higher in size) is less. As the duration of the test increases, deformation at the asperities increases the true area of contact of mating surfaces and also makes additional asperities (lower in size) on either specimen surfaces come in contact facilitating self-welding in more areas. Thus with increase in test duration, the breakaway shear stress required to separate the self-welded surfaces also increases.

4.4. Empirical relation

From the results obtained from the experiments, empirical relation between self-welding coefficient W and duration t were established for alloy D9 and 316LN as follows:

$$W = 0.0067\, t^{1/2} \quad \text{for annealed 316LN} \qquad (6)$$

$$W = 0.0013\ t^{1/2} \quad \text{for 20\% cold-worked 316LN} \quad (7)$$

$$W = 0.0 \quad \text{for annealed alloy D9} \quad (8)$$

$$W = 0.0020\ t^{1/2} \quad \text{for 20\% cold-worked alloy D9} \quad (9)$$

These relations can be used to predict whether the self-welding of the mating surfaces of various components in the rector can occur it their life time.

4.5 Surface damage due to self-welding

The surface of the self-welded specimens is examined by SEM. Fig. 4.3 shows a typical surface damage caused by self-welding in 20% cold-worked alloy D9 after testing for 6 months at 9.4 MPa in flowing sodium at 823 K (550°C). Surface damage observed in 20% cold-worked alloy D9 after the test of duration 4.5 months at contact stress of 24.5 MPa is shown in Fig. 4.4.

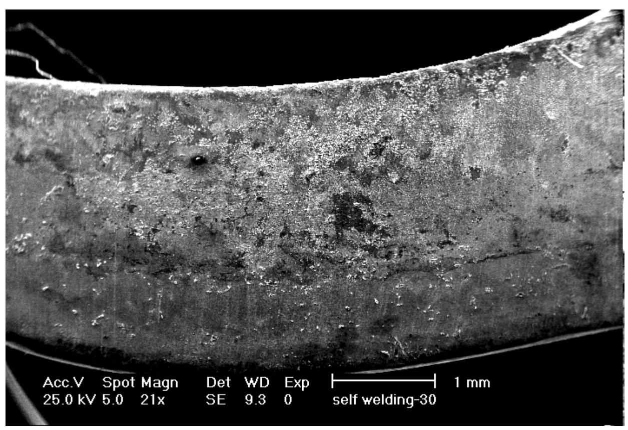

Fig. 4.3: SEM micrograph showing surface damage in self-welded region of a 20% cold-worked alloy D9 after testing for 6 months at 9.4 MPa in flowing sodium at 823 K

In contrast no damage is observed in the annealed alloy D9 tested for identical conditions (Fig. 4.5). Machine marks on the specimen remain more or less intact even after the test. For 316LN steel, the surface damage is more severe in the case of annealed steel tested for duration of 3 months at contact stress 12 MPa than in the case of 20% cold-worked material tested for 3 months at higher contact stress of 24.5 MPa as shown in Fig. 4.6 and 4.7 respectively.

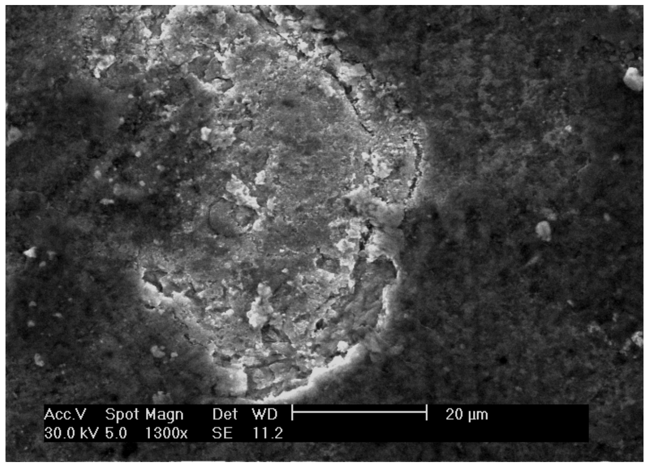

Fig. 4.4: SEM micrograph 20% cold-worked alloy D9 after 4.5 months in flowing sodium at 823 K with contact pressure 24.5 MPa

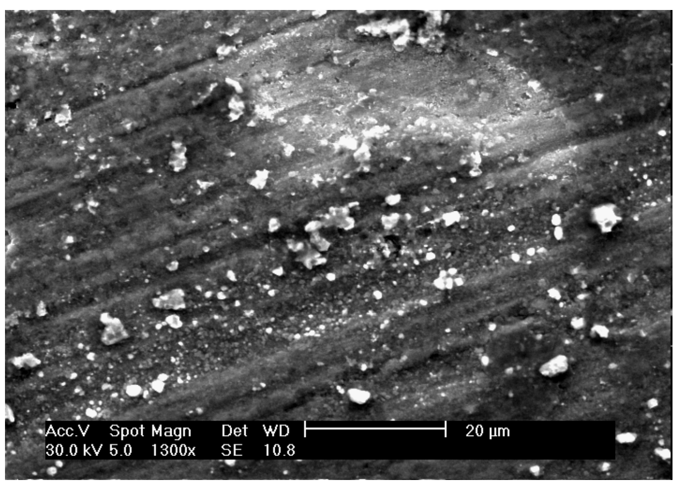

Fig. 4.5: SEM micrograph of annealed alloy D9 after 4.5 months in flowing sodium at 823 K with contact pressure 24.5 MPa

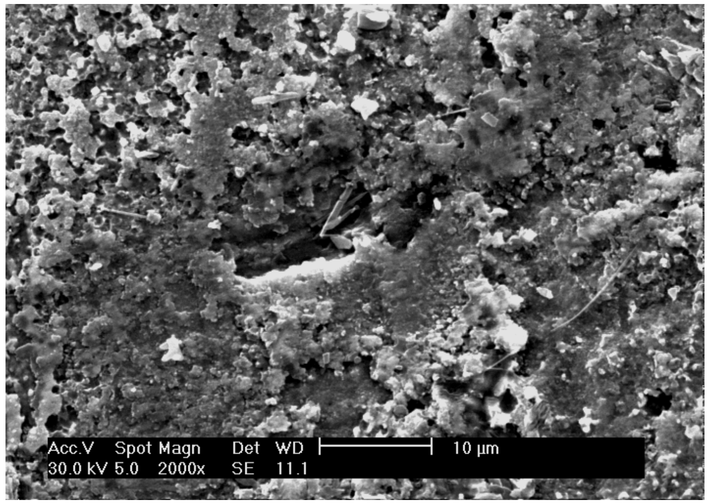

Fig. 4.6: SEM micrograph annealed 316LN after 3 months in flowing sodium at 823 K with contact pressure 12 MPa

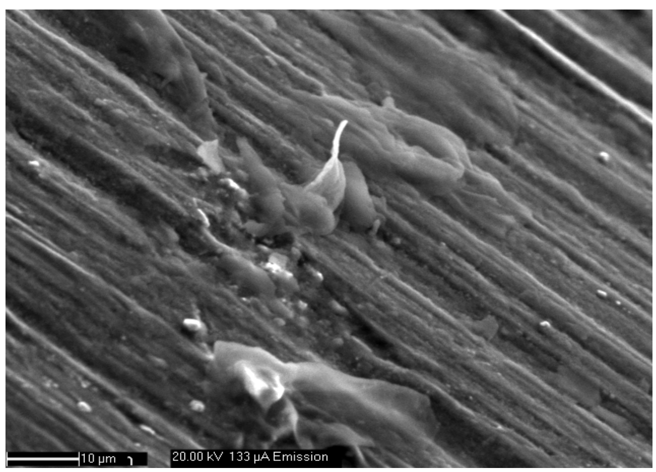

Fig. 4.7: SEM micrograph of 20% cold-worked 316LN after 3 months in flowing sodium at 823 K with contact pressure 24.5 MPa

4.6. Elemental analysis by Energy Disperse X-Ray Spectroscopy (EDS)

Though the specimens were cleaned from sodium after the test, some traces of sodium will be left behind on the surface of specimen. If a particular point is self-welded no sodium trace will be seen in EDS as this will be fresh surface produced during separation of the self-welded specimen, an operation carried out in air after the complete removal of the sodium. Accordingly EDS did not show sodium on annealed 316LN tested for 3 months indicating self-welding in this location as shown in Fig. 4.8. Presence of sodium in 20% cold-worked alloy D9 specimen tested for 3 months supports the observation that no self-welding at the location as shown in Fig. 4.9.

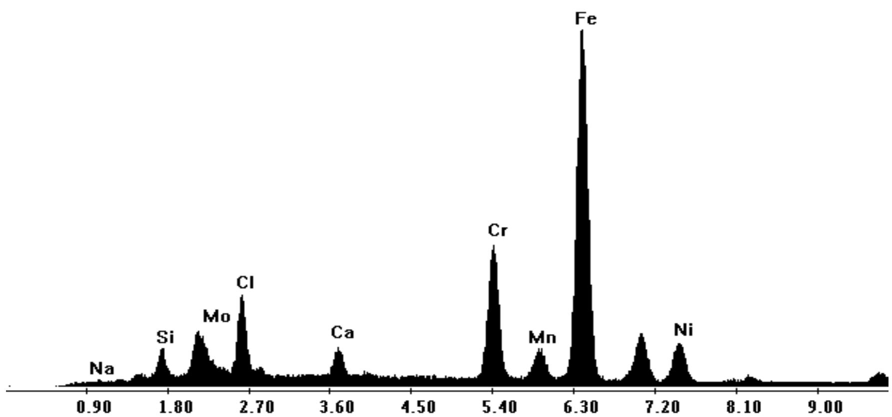

Fig. 4.8: Elemental counts by EDS in the self-welded region of annealed 316LN after testing for 3 months in flowing sodium at 823 K

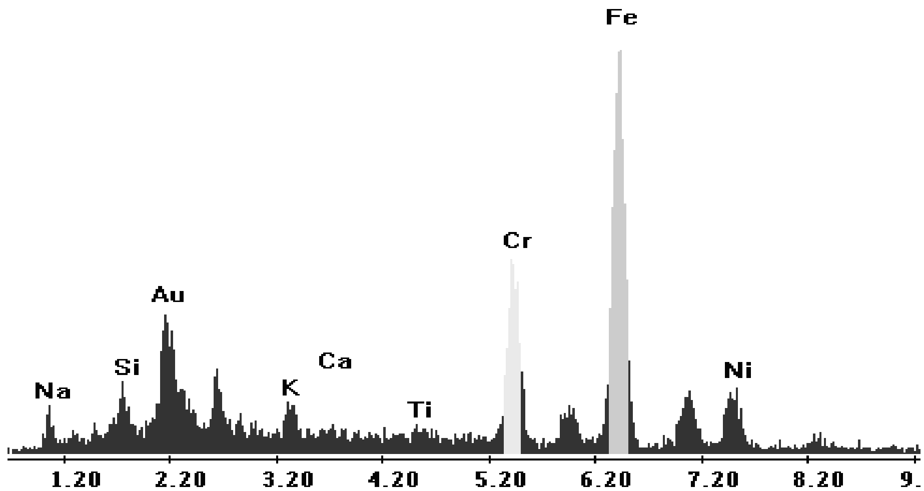

Fig. 4.9: Elemental counts by EDS in the 20% cold-worked alloy D9 after testing for 3 months in flowing sodium at 823 K

4.7. Microstructure and Hardness after self-welding susceptibility test

The microstructures of the specimens after self-welding tests are shown in Fig. 4.10. Comparing with the microstructure of the specimens before self-welding tests (Fig. 4.1) it is found that high twin density observed in cold-worked specimen before test has come down substantially after the test.

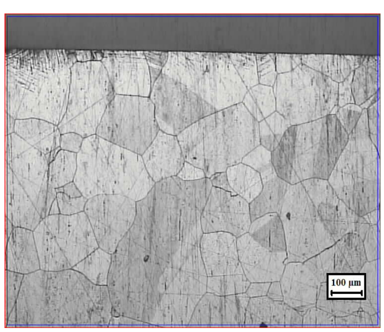

Annealed 316LN after 3 months

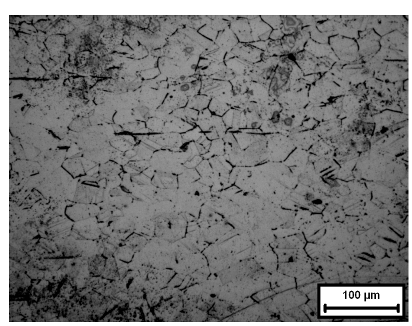

20% cold-worked 316LN after 4.5 months

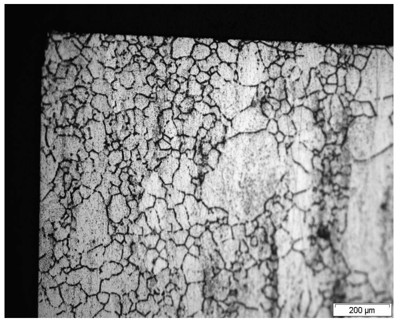

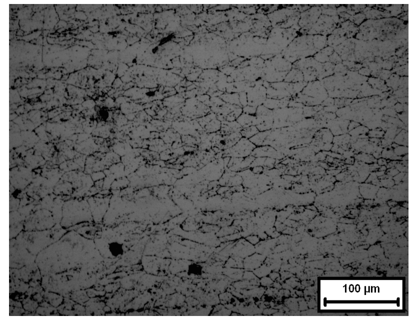

Annealed D9 after 4.5 months

20% cold-worked alloy D9 after 4.5 months

Fig. 4.10: Microstructure specimens after self-welding susceptibility studies in flowing sodium at 823 K

Table 4.4: Bulk Hardness (VHN) before and after self-welding tests

Material	Before test	After 3 months test	After 4.5 months test
Annealed D9	134±1	152±1	200±1
20%cold-worked D9	238±1	246±1	258±1
Annealed 316LN	145±1	133±1	-
20%cold-worked 316LN	265±1	263±1	259±1

Hardness of the specimens is measured before and after the test using Vickers hardness tester and results are shown in Table 4.4. It appears that 316LN showed a slight decrease in hardness after the test whereas alloy D9 showed slight increase in hardness after test. These results are in agreement with the results reported [23] in literature that temperature of 823 K (550°C) is not sufficient for recrystallisation of the cold-worked microstructure of these steels and prolonged exposure of the cold-worked alloy at this temperature did not result in any hardness change.

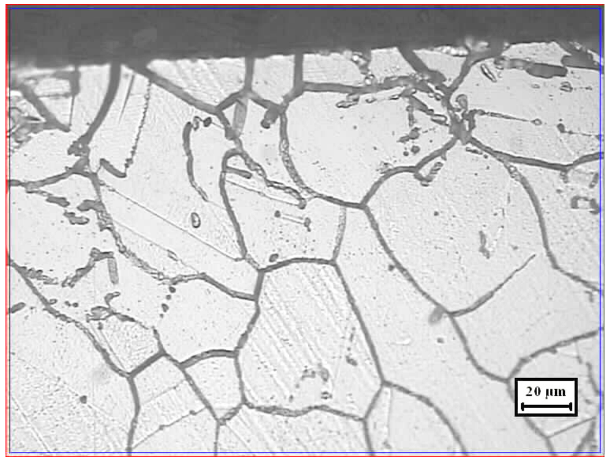

Fig. 4.11: Microstructure taken perpendicular to the mating surface (just below) of annealed alloy D9 specimen, after testing for 3 months in flowing sodium at 823 K

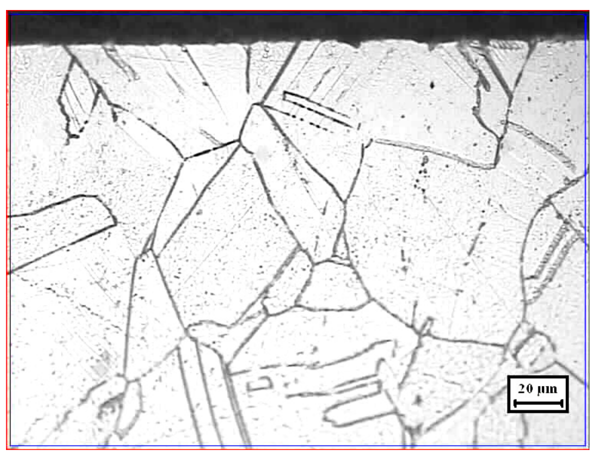

Fig. 4.12: Microstructure taken perpendicular to the mating surface (just below) of 20% cold-worked alloy D9 specimen, after testing for 3 months in flowing sodium at 823 K

A careful comparison of the microstructure close to the surface and away from it for specimens examined after completion of the test revealed that the grain boundaries are thicker near the surface. This is shown in Fig. 4.11 and 4.12 for annealed and 20% cold-worked alloy D9 respectively. This could be attributed to precipitation of carbides along the grain boundaries and the possible reason for this could be higher carbon content near the surface than away from it which in turn could be due to pick up of carbon from the sodium. If so, carbon content in the sodium exposed specimens near the surface shall be higher than that of the material which is not exposed to sodium. This is confirmed by the Auger electron spectroscopy (AES) carried out on alloy D9 specimens, results of which is shown in Fig. 4.13. It is found that there is an increase in carbon peak C indicating carburisation on the surface of specimens which were exposed to flowing sodium during the self-welding susceptibility test. Further, as seen from the microstructures shown in Fig. 4.11 and Fig. 4.12, carburization is more in annealed alloy D9 than in cold-worked alloy D9.

Microstructure of 20% cold-worked alloy D9 is examined under SEM to find out whether there is any change in the microstructure on that part of the specimen surface which is in contact with mating surface of the other specimen and the remaining part of the surface which is exposed to flowing sodium throughout the test. Figure 4.14 shows SEM micrographs of the specimen surface at locations C (which is in contact with mating surface of the other specimen) and E (which is not in contact with any other specimen).

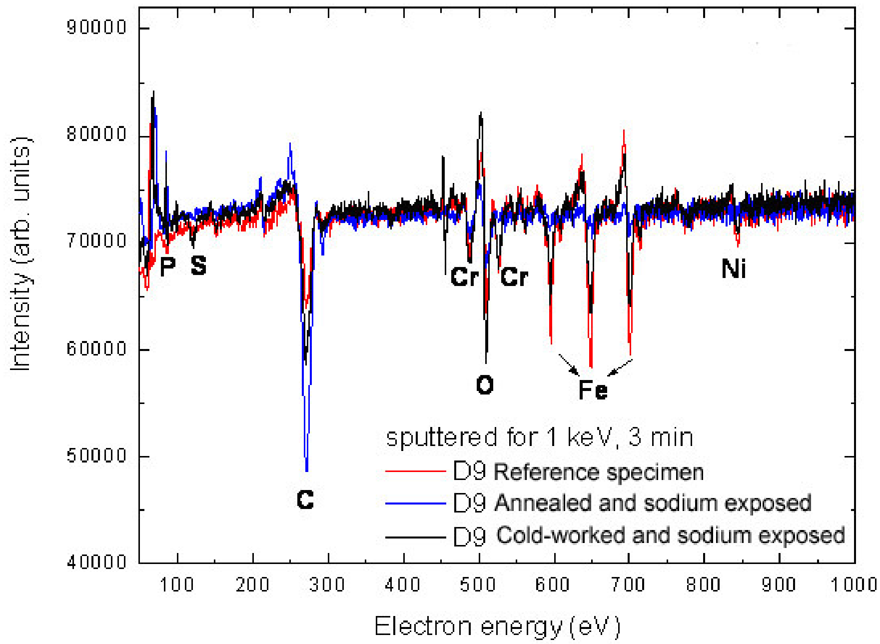

Fig. 4.13: AES spectra of reference D9, annealed D9 and 20% cold-worked D9 samples taken from 3 months tests

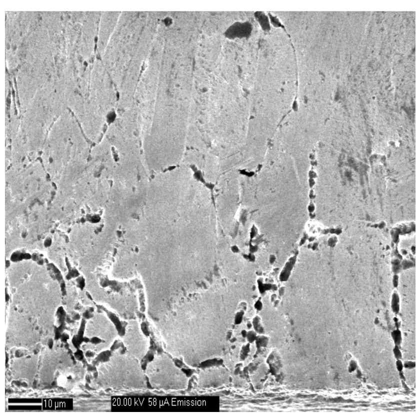

(a) SEM micrograph at point C which is under direct load

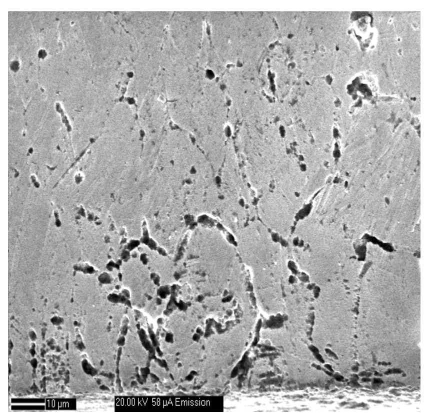

(b) SEM micrograph at point E which is not under load

Fig. 4.14: SEM micrograph of 20%cold-worked specimen after 4.5 months at 823 K in flowing sodium at 24.5 MPa contact pressure.

There is no change in carbide distribution observed along the grain boundaries at both these locations. Hence it is concluded that carbon pick up at the specimen surface is uniform and is not affected by the contact of the specimens at the mating surface.

4.8. Dynamic recrystallisation in cold-worked alloy D9

As the annealed alloy D9 is not susceptible to self-welding, the cold-worked alloy D9 with its higher hardness is expected to have maximum resistance to self-welding. However, results obtained are not in agreement with this. Microstructure of the materials at the location of self-welding is compared with similar location of the specimen where there is no self-welding. For this purpose metallographic samples were extracted from the self-welded test specimens as described in Fig. 3.13. In this sample, location marked C and D are in direct contact with test specimen and thus experiencing direct loading and higher stress during the self-welding susceptibility test. The location marked C corresponds to the location of self-welding. Location E is not in contact with specimen and does not experience direct loading and thus it is not under stress. Microstructures of the specimen at location C and E for cold-worked alloy D9 are shown in Fig. 4.15(a). Below the location C (self-welded) significant recrystallisation of the cold-worked structure has taken place for several microns depth in cold-worked alloy D9. At location E for cold-worked alloy D9 there is no recrystallisation. Since only the stressed point C is self-welded in high temperature flowing sodium, reason for self-welding is attributed to dynamic recrystallisation taking place on cold-worked alloy D9.

In contrast, in cold-worked 316LN no such recrystallisation is observed at C or E as shown in Fig. 4.15(b). No change in microstructure is observed with distance from the location of self-welding along the depth. This indicates that there is no dynamic recrystallisation in cold-worked 316LN. This could be the reason for better resistance of cold-worked 316LN to self-welding than for the cold-worked alloy D9.

At location C

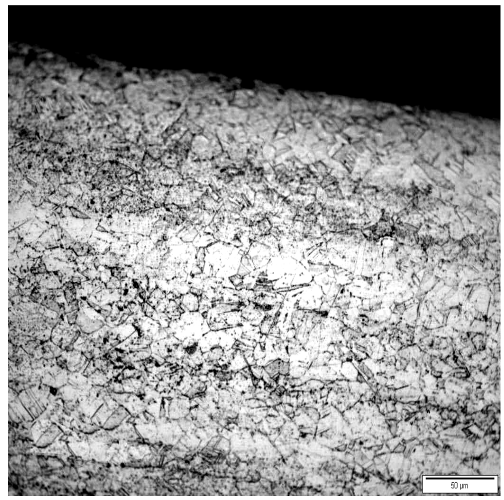

At location E

Fig. 4.15 (a): Microstructure just below the location of self-welding for of 20%cold-worked alloy D9 after 4.5 months in 823 K flowing sodium at 24.5 MPa contact pressure

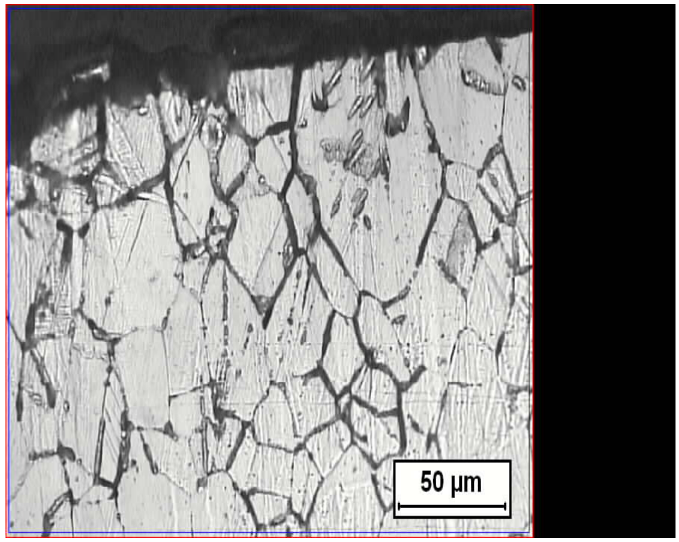

Fig. 4.15 (b): Microstructure just below the location of self-welding for of 20%cold-worked 316LN after 4.5 months in 823 K flowing sodium at 24.5 MPa contact pressure

Table 4.5: Hardness (VHN) of 20% cold-worked alloy D9 after 4.5 months test along the depth of specimen

	Hardness (VHN) of 20% cold-worked alloy D9		
Depth (mm)	**At point C (Direct loading)**	**At point E (No direct loading)**	**At point D (Direct loading)**
0.2	234	291	210
0.4	217	265	214
0.6	238	278	207
0.8	223	259	187
1	204	242	196

Table 4.6: Hardness (VHN) of 20% cold-worked 316LN after 4.5 months test along the depth of specimen

	Hardness (VHN) of 20% cold-worked 316LN		
Depth (mm)	**At point C (Direct loading)**	**At point E (No direct loading)**	**At point D (Direct loading)**
0.2	263	257	250
0.4	254	258	252
0.6	255	275	265
0.8	263	272	261
1	265	253	259

Microstructural change observed is also in line with hardness variations at locations C, D and E as measured using micro hardness tester, which are shown for cold-worked alloy D9 and cold-worked 316LN in Tables 4.5 and 4.6 respectively. It is clear that hardness for a depth of 1mm just below at location C and D is much lower than that at location E for the cold-worked alloy D9 (Table 4.5). At location C it is in the range of 200-240 VHN, at D it is in the range of 190- 215 and at E, it is in the range of 240-290. Hardness measured at location below E is close to the bulk hardness of 258 VHN for cold-worked alloy D9 reported in Table 4.4. In contrast, there is no specific change in hardness for locations C, D, E for cold-worked 316LN. For all the three locations, hardness measured are in a narrow range of 250-275 VHN [Table 4.6] which conforms to bulk hardness of 259 VHN reported for cold-worked 316LN after the test (Table 4.4).

From the results presented above, it can be concluded that dynamic recrystallisation that take place in cold-worked alloy D9 just below the mating surface is the reason for higher susceptibility to self-welding than the cold-worked 316LN. The reason for proposing this as dynamic recrystallisation is that it takes place when both stress and temperature act together. Hardness and microstructural changes are also confined only to the location just below the stressed part of the surfaces where self-welding had taken place. In the case of normal recovery and recrystallisation, hardness reduction and microstructural changes should have taken place throughout the test specimens. Further, recovery and recrystallisation studies carried out on alloy D9 at different temperatures indicate recrystallisation does not take place in the cold-worked alloy D9 at 823 K, the temperature of testing in the present study [23]. It should also be noted that though the nominal stress applied for self-welding susceptibility is low (24.5 MPa), the actual stress at the points of contacts of the mating surfaces (asperities present on the surfaces) would be high enough for dynamic recrystallisation to occur.

4.9. Precipitation of TiC in cold-worked alloy D9

Though alloy D9 and 316LN are austenitic stainless steels with almost similar composition, results presented here indicate that there is a significant change in the dynamic recrystallisation behavior of these two steels subjected to identical cold-work. Hence, literature available on recrystallisation behavior of alloy D9 is critically reviewed and it is found that recrystallisation in alloy D9 is influenced by presence of coarse TiC particles [24]. Ti is an alloying element only in alloy D9 and not in 316LN and composition of the alloy D9 is designed not to have coarse carbides in the steel in solution annealed and cold-worked condition. Only during high temperature exposure in service fine TiC are expected to be precipitated in this steel. Prolonged exposure of alloy D9 to flowing sodium results in pickup of carbon from liquid sodium and this facilitate the precipitation of TiC at locations close to the surface. Subsequent to coarsening of these precipitates, dynamic recrystallisation of cold-worked alloy D9 under stress can begin in the interface. Dynamic recrystallisation allows diffusion of atoms across the mating surfaces and as a result self-welding of the mating surfaces takes place.

To support this argument, it is necessary to show the presence coarse TiC among the carbides precipitated along the grain boundaries in the recrystallised zone of the specimen. To prove this in the present study, SEM-EDS analysis is carried out on the metallographic sample extracted from the cold-worked alloy D9 specimen, from the location corresponding to C in Fig 3.13, where self-welding is observed after the test. Figure 4.16 shows the SEM micrograph along with EDS spectra from two grain boundary carbides marked M and N in the micrograph. The precipitate marked M, which appears to be fairly coarse and few microns in size is rich in Ti indicating this is TiC. This means coarse TiC can be formed in alloy D9 surface due to pickup of carbon by the steel from flowing liquid sodium. These carbides can in turn facilitate dynamic recrystallisation of the cold-worked structure at the locations where the mating surfaces are under stress leading to self-welding of the surfaces at these locations.

4.10. Conditions favoring self-welding in cold-worked alloy D9

Thus, based on the facts that Ti is an alloying element present only in alloy D9, carburization of the cold-worked alloy D9 surface by flowing sodium can lead to precipitation of TiC at grain boundaries and coarse TiC precipitates can accelerate dynamic recrystallisation in cold-worked alloy D9 under stress, and thus self-welding in 20% cold-worked alloy D9. In annealed D9 there is no recrystallisation of cold-worked microstructure and hence, carburization of the surface by flowing sodium alone does not facilitate self-welding and hence it is resistant to self-welding.

As already stated, it is unlikely that TiC precipitates would be present in the alloy before the start of the test as it is in the solution annealed and subsequently cold-worked condition. It is formed while test is in progress and dynamic recrystallisation is expected to take place only after these precipitates are formed in the alloy. This would mean there could be an incubation time for self-welding to occur. In this context it may be noted that 20% cold-worked alloy D9 did not self-weld in the test durations of 3 months. Microstructural examination of the 3 months sample also did not reveal any evidence of dynamic recrystallisation, as coarse TiC is not available to facilitate dynamic crystallization in the short duration test.

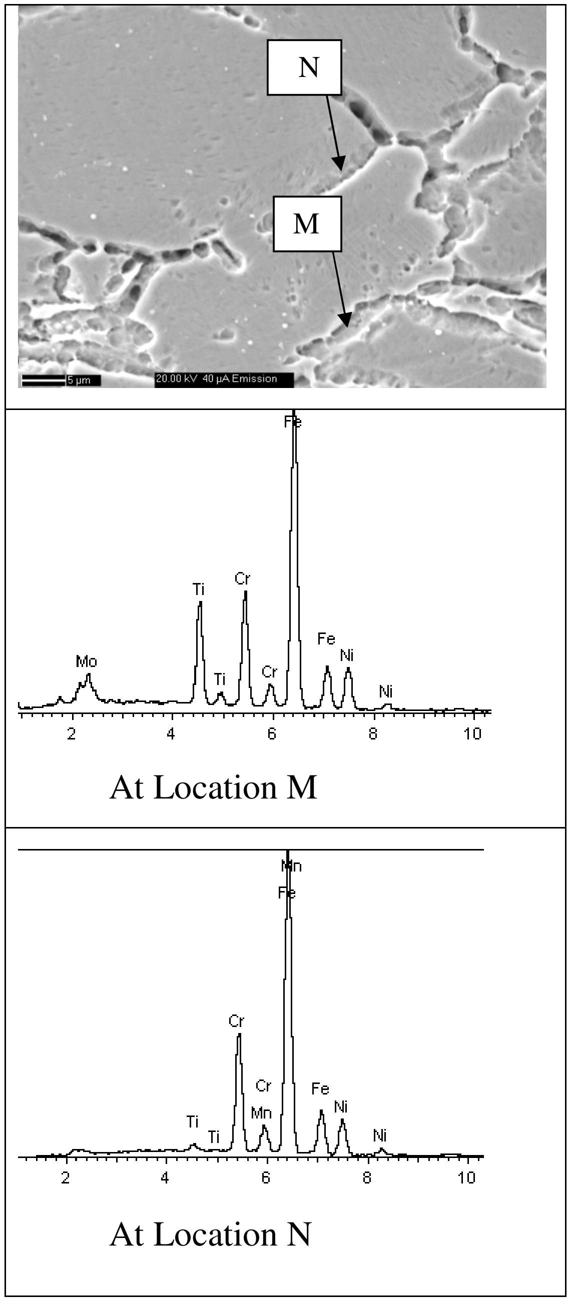

Fig. 4.16: SEM-EDS of 20% cold-worked alloy D9 after 4.5 months in 823 K flowing sodium at 24.5 MPa contact pressure

Another important aspect is the role of carburization of the alloy D9 by flowing sodium. If carbon in liquid sodium can be reduced further (from the present 25 ppm), then carburization of the specimen surface by flowing sodium may not take place and this also can indirectly prevent self-welding.

4.11 Summary

The self-welded specimen pairs are separated by a set up to measure the shear force. The tested specimens were later analyzed for self-welding using self-welding coefficient, SEM, EDS, Microstructure Macro and Micro hardness results. Empirical relations were derived for alloy D9 and 316LN in annealed and cold-worked condition. The SEM micrographs were presented showing the surface damage in all cases tested. The results indicated that the self-welding tendency is more in annealed 316LN than in 20% cold-worked 316LN which is on the expected line. On the contrary, 20% cold-worked alloy D9 showed more self-welding tendency and the annealed alloy D9 showed no self-welding. On analysis it was found that dynamic recrystallisation favoured self-welding tendency in 20% cold-worked alloy D9 and there was no dynamic recrystallisation in annealed alloy D9. The carburisation of alloy D9 in sodium resulted in the formation of TiC precipitates at the grain boundary near the surface which accelerated the dynamic recrystallisation in 20% cold-worked alloy D9. Thus 20% cold-worked alloy D9 was found to be more susceptible for self-welding in flowing sodium. It was also determined that for PFBR conditions, self-welding will not occur in 20% cold-worked alloy D9 contact pads of the subassemblies during its operation.

CHAPTER 5

CONCLUSIONS

5. CONCLUSIONS

5.1. Conclusions

Following are the major conclusions drawn from the study carried out on self-welding susceptibility for two austenitic stainless steels, alloy D9 and 316LN both in annealed and 20% cold-worked condition in flowing sodium:

- The accelerated test confirmed that self-welding of the fuel subassembly contact pads is unlikely to take place during the life time of the subassemblies in PFBR.
- The cold-worked alloy D9 is more susceptible to self-welding than cold-worked 316LN in flowing sodium at 823 K.
- Susceptibility of annealed 316LN steel is similar to that reported for other austenitic stainless steels like 321 and 304. However annealed alloy D9 did not show self-welding in flowing sodium for the stress levels, temperature and duration studied.
- High self-welding susceptibility of 20% cold-worked alloy D9 in flowing sodium is attributed to dynamic recrystallisation of the cold-worked structure in the presence of the applied stress. The dynamic recrystallisation is also accelerated by coarse TiC formed during testing due to pick up of carbon (present as impurity) from the flowing sodium.
- Dynamic recrystallisation is not observed in cold-worked 316LN specimens under these conditions of testing.

5.2. Scope for future work

5.2.1. *Long term tests for PFBR contact pads*

The results of this study indicate that self-welding of cold-worked alloy D9 specimens is assisted by dynamic recrystallisation, which is in turn linked to presence of coarse TiC precipitates at the location of self-welding. Formation of TiC in the steel is linked to carbon pick up from the flowing sodium and this is a time dependent phenomena. Hence, there could be a time threshold below which self-welding does not occur. Hence, there is a need to carryout tests for longer duration and at lower stress levels than those employed in the present study to confirm our observation that self-welding is unlikely to take place in the contact pads of fuel subassemblies of the PFBR during their resident time in the reactor.

5.2.2. Self-welding tests in sodium with low carbon

Results of this study indicated that carbon pick up from flowing sodium has significant role in the observed susceptibility of cold-worked alloy D9 to self-welding. If the carbon content in the liquid sodium is reduced below than that is present in the sodium (25 ppm) in the present study, it should be possible to minimize the risk of self-welding. This can be confirmed by carrying out the tests in sodium with lower carbon content thus establishing the maximum permissible carbon content in liquid sodium to avoid the risk of self-welding for 20% cold-worked alloy D9.

REFERENCES

REFERENCES

1. Rodriguez P, Bhoje S.B, *The FBR Program in India.* Energy, 1998, Vol. 23, Iss. 7-8, pp. 629- 636.
2. Chetal S.C, Balasubramanian V, Chellapandi P, Mohanakrishnan P, *The Design Of The Prototype Fast Breeder Reactor.* Nuclear Engineering and Design, 2006, Vol.236, pp.852.
3. Kale R.D, Rajan M. *Developments in Sodium Technology Current Science,* 2004, Vol.86, Iss.5, pp.668-675.
4. Chander S, Meikandamurthy C, Kale R. D, Krishnamurthy R. , *Experimental study of self-welding of materials in high temperature liquid sodium*, Wear 162-164 (1993) 458-465
5. Bhaduri AK, Indira R, Albert SK, Rao, BPS, Jain SC, Asokkumar S. *Selection Of Hardfacing Material For Components Of The Indian Prototype Fast Breeder Reactor*. Journal Of Nuclear Materials, 2004, Vol.334 , pp.109-114.Elsevier Science
6. Hemant Kumar, Ramakrishnan V, Rajan Babu V, Vijayashree R, Albert, S.K, Sritharan R, Meikandamurthy C, Balasubramaniyan V, Bhaduri A.K, *In-sodium Tribological Studies Pertaining to Core and Reactor Assembly Components for PFBR*, DAE-BRNS theme meeting on Nuclear Tribology, BARC, Mumbai, Oct 2007.
7. Venkadesan, S, Bhaduri AK, Rodriguez P, Microstructural stability of cold-worked titanium modified austenitic stainless steel. International conference on fast reactor core and fuel structural behaviour. Inverness (United Kingdom). 4-6 Jun 1990.
8. Surendran CS, Jose Varghese, Raghupathy S, Chellapandi P,

Engineered Safety Features To Avoid Dropping Of Core Subassemblies By Transfer Arm. International Journal Of Applied Engineering Research, 2011, Vol.6 ,Iss.5 , pp.777-784.

9. Bindu Sankar, Jaideep Chakraborty, Rashmi Nawlakha, Venkatesan A, Raghupathy S, Jayanthi, T, Satya Murty SAV. *Modelling and Simulation of In-vessel Core Handling In Pfbr Operator Training Simulator*. World Academy of Science, Engineering and Technology, 2012, Vol. - , Iss.67, pp.269-276.
10. Mannan S.L, Chetal S.C, Baldev Raj, Bhoje S.B *Selection Of Materials For Prototype Fast Breeder Reactor* Transactions Of The Indian Institute Of Metals, 2003, Vol.56, Iss.2, pp.155-178.
11. Chetal S.C, Bhoje S.B, Govindarajan S, Mannan SL, Paranjpe, SR, Rodriguez P, Venkadesan S *Stainless Steel Application in Prototype Fast Breeder Reactor, Stainless Steels Processing and Metallurgy* INCOSS-89: International Conference on Stainless Steels, Bombay , Feb.2-4, 1989
12. Hemant Kumar, Albert S.K., Bhaduri A.K, Meikandamurthy C, *Need for hard facing coatings on Wrapper pads of fuel subassemblies* PFBR/30000/GN/1052 April 2004
13. Bendorf K. *Experimental investigations of self-welding of structural materials under sodium* Nuclear Engineering and Design 14 (1970) 83-98
14. Huber F, Mattes K , *Investigations into self-welding of metallic materials,* Proc. International Conference on Liquid Metals Technology in Energy Production, Champion, Pennsylvania, USA (1976) 177-183
15. Ji Young Chang and Shields S.A, *Self-welding evaluation of Co-Cr-W*

(Stellite) alloys in sodium in J M Dahlke(ed), Proc Second Int. Conf. on Liquid Metal Technology in Energy Production, NTIS ,Springfield 1980 pp 3-19 3-26

16. Yukota N, Shimoyashiki S, *Investigation of Self-welding rate of structural materials in liquid sodium,* Nuclear Technology, 81 (1988) 407-414.

17. P. Agostini, E. Masetti, *Friction tests of PEC reactor elements prototypic specimens with sodium and air,* Liquid Metals Technology in Energy Production, 501 (1988) 1-9

18. Yoshida E, Hirakawa Y and Nihei I, *In-sodium tribological study on cobalt–free hard facing materials for contact and sliding parts of FBR components,* Proc. Conference on Liquid Metal Technology Avignon, Societe Francaise d'Energie Atomique, Paris (1988) 502-1 502-10.

19. Hemant Kumar, Albert S K, Ramakrishnan V, Meikandamurthy C, Vijayshree R, Bhaduri A.K *In-sodium self-welding susceptibility evaluation of chromium plated 2.25 Cr-1 Mo steel with Inconel 82 weld metal* in Int Journal Nuclear Energy Science and Technology Vol.3 No.4 2007 386-398

20. C.Meikandamurthy, M.Rajan *Design of self-welding test vessel* IGC / FRTG/ 3130/DN/1052 April 1998

21. C.Meikandamurthy, M.Rajan *Design of separation set up for self-welded pairs* IGC/FRTG/3130/DN/1053 Dec 1998

22. K.Gurumoorthy, KK Rajan Operation Procedure for BIM sodium loop IGC/ FRTG/3130/ OP/823 Rev April 1990

23. Venkadesan S, Bhaduri A.K Rodriguez P and Padmanabhan K.A, *Effect of ageing on the microstructural stability of cold-worked titanium-modified 15Cr-15Ni-2.5Mo austenitic stainless steel*, Journal

of Nuclear Materials, 186 (1992) 177-184

24. Vasudevan M, Venkadesan S, Sivaprasad P.V *Influence of Ti (C+6/7N) ratio on recrystallisation behaviour of cold-worked 15Cr-15Ni-2.2Mo-Ti modified austenitic stainless steel*, Journal of Nuclear materials, 231 (1996) 231-241.

ADDITIONAL REFERENCES

Baldev Raj, Chellapandi P, and Chetal SC *Sodium Cooled Fast Reactors: Technological Challenges And Opportunities* Science And Culture, 2013, Vol.79, pp.92-101 Elsevier.

Selvaraj A, Balasubramaniyan V, Raghupathy S, Elango D, Sodhi BS, Chetal SC, and Bhoje SB *Conceptual design of reactor assembly of prototype fast breeder reactor.* Technical committee meeting on conceptual designs of advanced fast reactors, Kalpakkam (India) 3-6 Oct 1995.

Puthiyavinayagam P, Roychowdhury DG, Govindarajan S, and Chetal SC *Design of PFBR Core Subassemblies.* Int Conf on Characterisation and Quality Control of Nuclear Fuels (CRCNF-2002), Dec 10-20, 2002, Hyderabad.

Sodhi BS, Sulekh Chander, Chetal SC, Selvaraj A, Kohli AK, and Rajesh Chandra *Conceptual design of core component handling system in PFBR.* Technical committee meeting on conceptual designs of advanced fast reactors. Kalpakkam (India) 3-6 Oct 1995.

Chetal SC, Mannan SL, Ray SK, Seetharaman V, and Srinivasan G, *Stainless Steel for Prototype Fast Breeder Reactor*. National Seminar on Stainless Steel, Salem, December 1982.

Indira R *Choice of hardfacing materials for LMFBR components*, Proceedings of thirteenth national symposium on radiation physics recent advances and future scenarios in accelerator radiation physics, Mumbai, India 1999 p 459-464.

Venkatraman B, Menaka M, Subbaratnam R, and Baldev Raj *Characterisation of Colmonoy Coatings using Lock-In Thermography* 17th World Conference on Nondestructive Testing, 25-28 Oct 2008, Shanghai, China.

Govindarajan S, Puthiyavinayagam P, and Bhoje S.B *Design implications of core mechanical behaviour*, Specialists' meeting on predictions and experience of core distortion behaviour. Wilmslow (UK). 1-4 Oct 1984.

Vaidyanathan G, Om Pal Singh, Govindarajan S, Chellapandi P, Chetal S.C, Shankar Singh R, and Bhoje S.B *Safety considerations in the design of PFBR*. Technical committee meeting on **c**onceptual designs of advanced fast reactors, Kalpakkam (India) 3-6 Oct 1995.

Puthiyavinayagam P, Roychowdhury D.G, Govindarajan S, and Chetal S.C, *Design of PFBR Core Subassemblies* International Conference on Characterisation and Quality Control of Nuclear Fuels (CRCNF-2002), Dec 10-20, 2002, Hyderabad.

Sodhi B.S, Sulekh Chander, Chetal S.C, Selvaraj A, Kohli A.K, and Rajesh Chandra, *Conceptual design of core component handling system in PFBR*. Technical committee meeting on conceptual designs of advanced fast reactors. Kalpakkam (India) 3-6 Oct 1995.

Puthiyavinayagam P, Ravichandar S.C, Chellapandi P, and Chetal S.C, *Design Criteria and Issues in Core Structural Materials of Sodium Cooled Fast Reactors* IAEA Technical Meeting, July 2 – 4, 2008, Hyderabad, India.

Mathew M.D, Venkadesan S, Sivaprasad P.V, Vasudevan M, Narayanan C, Shanmugam V, Venugopal S, Samuel K.G, Sandhya R, Latha S, Govindarajan, S, Rao KBS, and Mannan S.L *Development of Alloy D9 Stainless Steel and Evaluation of Mechanical Properties*. Seminar on Materials R&D for PFBR 2003, Kalpakkam India.

Bhoje S.B, and Govindarajan S *Bowing and interaction of fast reactor subassemblies* Bhabha Atomic Research Centre, Bombay (India) 1975.

Ganesan V *Corrosion of stainless steel in sodium and its contro*l. National symposium on electrochemistry in nuclear technology, Kalpakkam (India) 5-7 Jan 1994.

Ramakrishnan V *In-sodium tribological studies on hardfaced deposits* Theme meeting, IIM, Kalpakkam Chapter 11 Oct 2007.

Chetal, SC, and Chellapandi P, *Indian Fast Reactor Technology: Current Status And Future Programme* Sadhana, 2013, Vol.38, Iss.5, pp795-815 Springer.

Srinivasan R, Chellapandi P, and Chetal SC, *Comparison Of SS 304 LN And 316 LN As Choice Of Structural Material For Primary Pipe In Fast Breeder Reactors'* Transactions Of The Indian Institute Of Metals, 2010, Vol.63, Iss.1-2, pp 607-610 Springerlink.

Chellapandi P, Rajan Babu V, Puthiyavinayagam P, Chetal SC, and Baldev Raj, *Experimental Evaluation Of Integrity Of FBR Core Under Seismic Events. Journal Of Power And Energy Systems,* 2008, Vol.2, Iss.2, pp 582-589.

Chetal, SC, Chellapandi P, Puthiyavinayagam P, Raghupathy S, Balasubramanian V, Selvaraj P Mohanakrishnan P, and Baldev Raj *A Perspective on Development of future FBRs in India* Int. Conference on Fast Reactors and Related Fuel Cycles: Challenges and Opportunities (FR-09), 7-11 December 2009, Kyoto, Japan.

Chetal SC *Design and manufacturing aspects of components of Prototype Fast Breeder Reactor* OPE-AINDT Conference, Queensland, Australia, 26-28 August 2009.

Chetal SC, *Design to Ensure Long Plant Life with High Performance for Sodium Cooled Fast Reactors*. Workshop on Nuclear Power Plant Life Management, Kalpakkam, 6-9 October 2009.

Balasubramaniyan V, Puthiyavinayagam P, Chellapandi P, and Chetal SC, *Experiences with design and manufacture of Reactor Assembly Components of PFBR*. International Symposium on Advances Stainless Steels 2007 (ISAS

2007), Chennai, 09-11, Apr 2007.

Puthiya Vinayagam P, Clement Ravi Chandar S, Sivayya DN, Rajan Babu V, Chellapandi P, Chetal SC, and Baldev Raj, *Design Safety Limits for Fuel, Clad and Sodium under Different Design Basis Events for PFBR*. Indo – French Technical Meeting, IGCAR, Kalpakkam , 27 – 28, Feb 2006

Gupta, A, Chellapandi P, and Chetal SC *Seismic Behaviour of PFBR Core.* National Seminar on Seismic Design of Nuclear Power Plants, February 21-22, 2003, SERC, Chennai.

Kasinathan, N, Parthasarathy, U, Natesan K, Selvaraj P, Chellapandi P, Chetal SC, and Bhoje SB *Analysis of Design Basis Events for Prototype Fast Breeder Reactor.* 1st National Conference on Nuclear Reactor Safety, Mumbai, 25-27 Nov 2002.

Singh, OP, Chetal SC, Bhoje SB, *Safety Design of Prototype Fast Breeder Reactor.* 1st National Conference on Nuclear Reactor Safety, Mumbai, 25-27, Nov 2002.

Ghosh G, Puthiyavinayagam P, Ravichandar SC, Sridhar Rao MV, Ravichandran G, and Sahu RR *Thermal Hydraulic design of PFBR Core*. IAEA TCM on LMFBR core thermohydraulics: Status and prospects, Vienna, June 2000.

Gajapathy R, Selvaraj P, Chellapandi P, Chetal SC, and Bhoje SB, *Investigation of PFBR Spent fuel Clad Temperature during Handling*. ICONE-8, April 2-6, 2000, Baltimore, USA.

Roychowdhury DG, Govindarajan S, Chetal SC, and Bhoje SB, *Thermal Hydraulic Design of PFBR Core.* IAEA IWGFR Technical Committee Meeting on Methods and Codes for Calculations of Thermohydraulic Parameters for fuel, Absorber Pins and Assemblies of LMFRs with Traditional and Burner Cores, Obninsk, Russia, July 27-31, 1998

Vaidyanathan G, Om Pal Singh , Govindarajan S, Chellapandi P, Chetal SC, Shankar Singh R, and Bhoje SB *Safety considerations in the design of PFBR.* Technical committee meeting on conceptual designs of advanced fast reactors.Kalpakkam (India) 3-6 Oct 1995.

Selvaraj A, Balasubramaniyan V, Raghupathy S, Elango D, Sodhi BS, Chetal SC, and Bhoje SB *Conceptual design of reactor assembly of prototype fast breeder reactor.* Technical committee meeting on conceptual designs of advanced fast reactors. Kalpakkam (India). 3-6 Oct 1995.

Chetal SC, Bhoje SB, Govindarajan S, Mannan SL, Paranjpe SR, Rodriguez P, and Venkadesan S *Stainless Steel Application in Prototype Fast Breeder Reactor* Stainless Steels Processing and Metallurgy INCOSS-89: International Conference on Stainless Steels, Bombay , Feb.2-4, 1989

Chetal SC *Design and Fabrication Aspects of Stainless Steel.* Workshop on Stainless Steels, IIT, Chennai, December 1988.

Rodriguez P, Paranjpe SR, Chetal SC, Mannan SL, Ray SK, Seetharaman V, and Srinivasan G *Overview of fast reactor structural materials programme in India.* Specialists' meeting on mechanical properties of structural materials including environmental effects. Chester (UK) 10-14 Oct 1983.

Chetal SC, Mannan SL, Ray SK, Seetharaman V, and Srinivasan G, *Stainless Steel for Prototype Fast Breeder Reactor.* National Seminar on Stainless Steel Salem, December 1982

Sodhi BS, Sulekh Chander**,** Chetal SC, Selvaraj A, Kohli AK, and Rajesh Chandra *Conceptual design of core component handling system in PFBR.* Technical committee meeting on conceptual designs of advanced fast reactors. Kalpakkam (India). 3-6 Oct 1995.

Baldev Raj, Kamachi Mudali U, Vijayalakshmi M, Mathew MD, Bhaduri

AK, Chellapandi P, Venugopal S, Sundar CS, Rao BPC, and Venkataraman B *Development Of Stainless Steels In Nuclear Industry with Emphasis On Sodium Cooled Fast Spectrum Reactors*. Journal Of Advanced Material And Research, 2013, Vol.794, pp.3-25

Sumantra Mandal, Bhaduri, AK, and Subramanya Sarma, V *Influence Of State Of Stress On Dynamic Recrystallization In A Titanium-modified Austenitic Stainless Steel.* Metallurgical And Materials Transactions A: Physical Metallurgy And Materials Science, 2012, Vol.43, Iss.2, pp 410-414 Springer Boston, United States.

Kumar N, Das CR, Dash S Tyagi AK, Bhaduri AK, and Baldev Raj *Evaluation Of Tribological Properties Of Nuclear-grade Steel* Tribology Transactions 2011, Vol.54, Iss.1, pp 62-66.

Bhaduri AK, Albert SK, Shankar V, and Ray SK, *Welding And Hardfacing For The Prototype Fast Breeder Reactor.* Indian Welding Journal, 2006, Vol.39, Iss.2, pp18-31.

Bhaduri, AK, Indira, R Albert SK, Rao BPS, Jain SC, and Asokkumar S, *Selection Of Hardfacing Material For Components Of The Indian Prototype Fast Breeder Reactor*. Journal Of Nuclear Materials, 2004, Vol.334, pp.109-114 Elsevier Science.

Hemant Kumar, Ramakrishnan V, Rajan Babu V, Vijayashree R, Albert SK, Sritharan R, Meikandamurthy C, Balasubramaniyan V, and Bhaduri AK, *In-sodium Tribological Studies Pertaining to Core and Reactor Assembly Components for PFBR.* DAE-BRNS theme meeting on Nuclear Tribology, BARC, Mumbai, Oct 2007

Venkadesan S, Bhaduri AK, and Rodriguez P, *Microstructural stability of cold-worked titanium modified austenitic stainless steel.* International conference on fast reactor core and fuel structural behaviour, Inverness

(United Kingdom) 4-6 Jun 1990.

Bhoje SB *Rationale For The Fast Breeder Reactor*. Current Science 2002 Vol.83, Iss.5, pp 542-543

Bhoje SB, and Chellapandi P, *Advanced Structural Design Of High Temperature Components Of FBR*. Transactions Of The Indian Institute Of Metals, 2000, Vol. 53, Iss. 3, pp165- 173.

Rodriguez P and Bhoje SB, *The FBR Program In India*. Energy, 1998, Vol. 23, Iss.7-8, pp 629- 636.

Singh OP, Chetal SC, and Bhoje SB, *Safety Design of Prototype Fast Breeder Reactor* 1st National Conference on Nuclear Reactor Safety, Mumbai, 25-27, Nov 2002.

Bhoje SB, Sinha RK, and Sethi VK. *New Trends in Nuclear Power Technology*. The Economic Times Power India 2001 - 3rd Inte Conf. 21-23 Nov 2001, Mumbai.

Bhoje SB, Govindarajan S, and Puthiyavinayagam P *Emerging Trends in Fast Breeder Reactors*. 12th Annual Conf of the Indian Nuclear Society. 10-12 Oct 2001. Indore.

Gajapathy R, Selvaraj P, Chellapandi P, Chetal SC, and Bhoje SB. *Investigation of PFBR Spent fuel Clad Temperature during Handling*. ICONE-8 April 2-6, 2000, Baltimore, USA.

Muralikrishnan, R, Chellapandi P, Chetal SC, and Bhoje SB *Dynamic Displacements of PFBR Core with Reference to Reactivity Oscillations during a Seismic Event* SMiRT-15, Seoul, Korea, 15-20 Aug 1999.

Bhoje SB and Govindarajan S, *The need and the role of nuclear energy in India* International seminar on nuclear power in developing countries: Its potential role and strategies for its deployment Mumbai (India) 12-16 Oct 1998

Vaidyanathan G, Om Pal Singh, Govindarajan S, Chellapandi P, Chetal SC, Shankar Singh R, and Bhoje SB *Safety considerations in the design of PFBR.* Technical committee meeting on conceptual designs of advanced fast reactors.Kalpakkam (India). 3-6 Oct 1995.

Lee SM, Govindarajan S, Indira R, John TM, Mohanakrishnan P, Shankar Singh R, and Bhoje SB *Conceptual design of PFBR core.* Technical committee meeting on conceptual designs of advanced fast reactors. Kalpakkam (India). 3-6 Oct 1995.

Puthiyavinayagam P, Gopal S, Winston SJ, Govindarajan S Chetal SC, and Bhoje SB, *Influence of swelling and creep data on PFBR core design.* Technical committee meeting on influence of high dose irradiation on core structural and fuel materials in advanced reactors Obninsk (Russian Federation) 16-19 Jun 1997.

Rodriguez P, Bhoje SB, and Lee SM *Reactor strategy for nuclear resource utilization in India.* International symposium on nuclear fuel cycle and reactor strategies: Adjusting to new realities Vienna (Austria) 3-6 Jun 1997.

Birsingh S, Govindarajan S, and Bhoje SB *Bowing and interaction model for sub-assemblies in a fast reactor core.* International seminar on containment of fast breeder reactors (CONFABRE-2). Berlin, Germany, 9 - 21 Aug 1979.

Rajan Babu V, Sritharan R, Vijayashree R, Balasubramaniyan V, Raghupathy S, Puthiyavinayagam P, Chellapandi P, and Chetal SC *Hard Facing on PFBR NSSS Components.* (SMT 23) Indian Institute of Metals, Kalpakkam Chapter, GRT, Mamallapuram, Nov 2-5, 2009.

Puthiyavinayagam, P, Ravichandar SC, Chellapandi P, and Chetal SC. *Design Criteria and Issues in Core Structural Materials of Sodium Cooled*

Fast Reactors. IAEA Technical Meeting on Status and Trends of Stainless Steel Cladding and Fuel Assembly Materials and Components for Liquid Metal Cooled Fast Reactor July 2 – 4, 2008, Hyderabad, India

Puthiyavinayagam P, Ravichandar SC, Chellapandi P, and Chetal SC *Design of PFBR Fuel Sub-assembly.* IAEA Technical Meeting on Status and Trends of Stainless Steel Cladding and Fuel Assembly Materials Kalpakkam 603102, TN, July 2–4, 2008

END